



Contents lists available at ScienceDirect

Journal of Quantitative Spectroscopy and Radiative Transfer

journal homepage: www.elsevier.com/locate/jqsrt

Partition sums for molecules and their isotopologues for HITRAN2024

Robert R. Gamache^{a,*}, Bastien Vispoel^b, Jonathan Tennyson^c, Sergei N. Yurchenko^c, Oleg L. Polyansky^{c,d}, Iouli E. Gordon^e, Robert J. Hargreaves^e, Xinchuan Huang^{f,g}^a Department of Environmental, Earth, and Atmospheric Sciences, University of Massachusetts Lowell, Lowell, MA 01854, USA^b Research Unit Lasers and Spectroscopies (LLS), Institute of Life, Earth and Environment (ILEE), University of Namur (UNamur), 61 rue de Bruxelles, Namur B-5000, Belgium^c Department of Physics and Astronomy, University College London, London WC1E 6BT, United Kingdom^d Institute of Applied Physics, Russian Academy of Sciences, Ulyanov Street 46, Nizhny Novgorod 603950, Russia^e Center for Astrophysics, Harvard-Smithsonian, Atomic and Molecular Physics Division, Cambridge, MA 02138, USA^f MS 245-6, Astrophysics Branch, Space Science and Astrobiology Division, NASA Ames Research Center, Moffett Field, CA 94035, USA^g SETI Institute, 339 Bernardo Ave, Suite 200, Mountain View, CA 94043, USA

ARTICLE INFO

Keywords:

Total internal partition sums

HITRAN2024

FORTRAN and python codes

ABSTRACT

Total Internal Partition Sums (TIPS), $Q(T)$, were calculated for four new isotopologues of molecules on HITRAN2020 ($^{16}\text{O}^{14}\text{N}^{18}\text{O}$, $^{14}\text{NH}_2\text{D}$, H^{13}COOH , $^{13}\text{CH}_3\text{F}$), for the five most abundant isotopologues of N_2O , for the two most abundant isotopologues of NO_2 , for the two most abundant isotopologues of NH_3 , the seven most abundant isotopologues of OCS , and the four most abundant isotopologues of CS_2 , and for six new molecules added to HITRAN2024: CH_3 , S_2 , COFCl (two isotopologues; $^{12}\text{C}^{16}\text{O}^{35}\text{Cl}$ and $^{12}\text{C}^{16}\text{O}^{37}\text{Cl}$), HONO , ClNO_2 (two isotopologues; $^{35}\text{ClNO}_2$ and $^{37}\text{ClNO}_2$), and H_3^+ (four isotopologues: H_3^+ , H_2D^+ , HD_2^+ , and D_3^+). The calculations for N_2 (J. Phys. Chem. Ref. Data 52, 023,101 (2023)) and NO (J. Phys. Chem. Ref. Data 53, 033,103 (2024)) were also added to TIPS2024. In addition, all partition sums on TIPS2020 (JQSRT 271 (2021) 107,713) calculated prior to 2020 were recalculated using the most recent CODATA constants (J. Phys. Chem. Ref. Data 50, 033,105 (2021)), while the differences are very small, TIPS2024 provides a consistent set of partition sums for all molecules/isotopologues on HITRAN2024. In total TIPS2024 provides data for 196 isotopologues of 62 molecules. The calculations range from $T = 1$ K to T_{max} , where the maximum temperature is determined based on the available energy states for a particular isotopologue that ensure convergence of $Q(T)$.

1. Introduction

There are many applications in physics and chemistry that depend on the total internal partition sums (TIPS). As such, there is a long history of providing TIPS [1–7] with new releases of the HITRAN database [8–15]. Here the concern is for systems that are in local thermodynamic equilibrium (LTE), however, work has been also done [16–18] for systems that are in non-local thermodynamic equilibrium. Using the TIPS and its first and second moments as a function of temperature, one can determine the equation of state of a gas, the thermodynamic functions (internal energy, enthalpy, entropy, Helmholtz free energy, and Gibbs free energy), heat capacity, etc. If the number density of molecules in a sample of gas is known, the TIPS can be used to determine the population of molecules as a function of the quantum state. These population factors are needed to determine the intensity, S , of ro-vibrational

transitions. The expressions that show the relationships between the intensity of a spectral line and the square of the transition moment, the Einstein-A coefficient, or the oscillator strength [19] all contain the partition sum.

The study of planetary and exoplanet atmospheres relies on the use of radiative transfer models, which require spectral input data, i.e. the line position, ω , lower-state energy, E' , intensity at a reference temperature, $S(T_{\text{ref}})$, and the half-width, γ , and line shift, δ , for the atmospheric pressure regimes. These parameters are found in molecular spectroscopic databases such as HITRAN [13,14] or GEISA [20]. The temperature and pressure vary in these atmospheres as a function of altitude and location (θ, ϕ), thus the temperature dependence of S, γ , and δ must be known. An accurate model of the temperature dependence of γ and δ was derived by Gamache and Vispoel in 2018 [21]. While HITRAN has adopted the Gamache and Vispoel model cutoff at two terms, most of

* Corresponding author.

E-mail address: Robert.Gamache@uml.edu (R.R. Gamache).<https://doi.org/10.1016/j.jqsrt.2025.109568>

Received 11 March 2025; Received in revised form 17 June 2025; Accepted 17 June 2025

Available online 18 June 2025

0022-4073/© 2025 Elsevier Ltd. All rights reserved, including those for text and data mining, AI training, and similar technologies.

the data for the half-widths remain in the power law form, $\gamma(T) = \gamma(T_{ref}) \left[\frac{T_{ref}}{T} \right]^n$, where n is called the temperature exponent. Note, only a limited amount of data are available for the temperature dependence of the line shift using a linear model [22,23] which only works over short temperature ranges [21]. The temperature dependence of the line intensity is given by [10]

$$S_{f \rightarrow i}(T) = S_{f \rightarrow i}(T_{ref}) \frac{Q(T_{ref})}{Q(T)} \frac{e^{-hcF''/kT}}{e^{-hcF''/kT_{ref}}} \frac{[1 - e^{-hc\omega_{f \rightarrow i}/kT}]}{[1 - e^{-hc\omega_{f \rightarrow i}/kT_{ref}}]} \quad (1)$$

where $Q(T)$ is the total internal partition sum, h and k are the Planck and Boltzmann constants, c is the speed of light, F'' is the lower state term value (hcF'' is the lower state energy, i.e. E_i), and $\omega_{f \rightarrow i}$ is the wavenumber of the transition. Thus, the partition sums allow the line intensities on HITRAN or GEISA to be propagated to other temperatures.

There are several compilations of partition sums for high temperature applications such as stellar atmospheres. Sauval and Tatum [24] calculated partition functions for roughly 300 diatomic molecules over a temperature range of 1000 to 9000 K. Irwin [25] refined their work for H_2 and CO and later calculated partition functions for polyatomic molecules [26] that significantly affect the stellar atmospheric equation of state. These works were of particular interest to the Joint-Army-Navy-Air Force (JANAF) program [27]. Barklem and Collet [28], in 2016, determined partition functions and dissociation equilibrium constants for 291 diatomic molecules for temperatures in the range from near absolute zero to 10 000 K. The ExoMol database [29] (<http://www.exomol.com/>) provides partition functions for 96 molecules with a broad coverage of temperatures, often up to 9000 K. There are many other examples of high-quality partition sums in the literature, often for one or several molecular isotopologues.

This work aims to extend TIPS2020 to consider all molecule/isotopologues on HITRAN2024, with the addition of a number of molecules/isotopologues not found in HITRAN2020 and updates to isotopologues of several molecules. The determination of partition sums for molecules/isotopologues on HITRAN began with the 1986 edition of HITRAN [8] when Gamache et al. [1] presented TIPS for the 11 closed-shell linear molecules. The $Q(T)$ data were given by polynomial expansions in two temperature ranges: 70–400 and 400–2005 K and a logarithmic expansion allowed extrapolation to 3000 K. This work was extended [2] to include all molecular/isotopologue species on HITRAN92 [9] and three additional molecular/isotopologue species from HITRAN96 [10]. The TIPS data were calculated 70 to 3005 K and for recall the data were divided into three temperature regions and each fit by a 3rd order polynomial. The work was extended in 2002 to consider 5 molecules (16 isotopologues) abundant in planetary atmospheres [3] (temperatures from 70–3000 K with 4th order polynomial fits to recall the data) and for Non-Local Thermodynamic Equilibrium (NLTE) applications [30] (temperatures from 70–450 K with 3rd order polynomial fits to recall the data). In 2003, calculations from 70–3000 K were made by Fischer et al. [4] for the 40 molecules and 95 isotopologues/isotopomers present on the HITRAN2000 database [31]. This work also included an additional 13 less abundant isotopologues/isotopomers of ozone and carbon dioxide. Recall of the data changed from the polynomial representation in different temperature ranges to a Lagrange 4-point interpolation scheme. In 2011, TIPS were calculated by Laraia et al. [5] for 14 molecules (33 isotopologues) needed to support planetary remote sensing. Some of the molecules of this study were later additions to HITRAN2020. The TIPS calculations were extended in 2017 to consider 24 molecules (73 isotopologues) added to HITRAN2016 [6]. In 2017 TIPS were reported for 181 isotopologues of 57 molecules important in planetary atmospheres [7]. Finally, in 2020 molecules number 1–55 were taken from the HITRAN2020 list, and for some molecules additional isotopologues were considered. New TIPS were calculated for 28 molecule/isotopologues

and the temperature range was 1–5000 K, with some molecule/isotopologues going to higher temperatures depending on the source of the term values. Also new in the work was the addition of a Python code to recall the TIPS. Each new edition of TIPS represents an improvement over the previous calculations.

In the literature, the terms “partition function” and “partition sum” are often interchanged. Here, the standard chemistry notation, $Q(T)$, is adopted for the total internal partition sum as a function of temperature, T . The total partition function is assumed to be the product of the internal and the translational partition functions.

Here, Total Internal Partition Sums were calculated for four new isotopologues of molecules on HITRAN2020 ($^{16}O^{14}N^{18}O$, $^{14}NH_2D$, $H^{13}COOH$, $^{13}CH_3F$), for the 5 most abundant isotopologues of N_2O , for the 2 most abundant isotopologues of NO_2 , for the 2 most abundant isotopologues of NH_3 , the 7 most abundant isotopologues of OCS, and the 4 most abundant isotopologues of CS_2 , and for seven new molecules added to HITRAN2024: CH_3 , S_2 , $COFCl$ (two isotopologues, $^{12}C^{16}O^{35}Cl$ and $^{12}C^{16}O^{37}Cl$), $HONO$, $ClNO_2$ (two isotopologues, $^{35}ClNO_2$ and $^{37}ClNO_2$), and H_3^+ (four isotopologues: H_3^+ , H_2D^+ , HD_2^+ , and D_3^+)... The calculations for N_2 [32] and NO [33] were also added to TIPS2024. To provide a consistent set of partition sums for all molecule/s/isotopologues on HITRAN2024, partition sums calculated prior to 2020 were recalculated using the most recent CODATA constants [34]. Note, propane, $^{12}C_3H_8$, which was in TIPS2020 as molecule 56 is not yet in HITRAN. With the addition of the new molecules, propane will now be labeled molecule 62 in TIPS2024.

Section 2 describes the calculation of total internal partition sums for the molecules/isotopologues new in this work. The methods used have been presented in previous publications [3–6,30] so only a quick overview is presented with appropriate references given. Section 3 describes the methods used to calculate $Q(T)$ for each molecule/isotopologue of this work. The codes to quickly recall the $Q(T)$ values are presented in Section 4 and, finally, Section 5 summarizes the work.

2. Determining the total internal partition sum

For a molecule in thermodynamic equilibrium, the total internal partition sum is given by summing the factor $e^{-hcF_s/kT}$ over all quantum states, s , of the molecule. The factor hcF_s is the total energy (electronic, vibrational, rotational, and any other quantized motion) of state s and F_s is the term value [35] (units of cm^{-1}), h is the Planck constant, c is the speed of light, k is the Boltzmann constant, T is the temperature in degrees Kelvin. The physical constants, h , c , and k are the CODATA recommended values [34]. If the energy states are degenerate, the sum needs to be done only once and multiplied by the degeneracy factor, of which some are state dependent; i.e. they depend on the quantum numbers of the state, d_s , or state independent; i.e. they are a factor given for the molecule, d_i . Adding the degeneracy factors, $Q(T)$, can be written as

$$Q_{elec, vib, rot, tors, etc.} = d_i \sum_{all\ states\ s} d_s e^{-hcF_s/kT} \quad (2)$$

The state-dependent degeneracy factors are generally composed of two components. The first is the usual $(2J+1)$ or $(2F+1)$ degeneracy factor, where J and F are the rotational and total angular momentum quantum numbers. For molecules where identical atoms are interchanged by a symmetry operation, only certain products of rotational and nuclear wavefunctions yield the proper symmetry for the complete wavefunctions. The result is that for some molecules/isotopologues, even and odd symmetry states have different nuclear spin weights that must be factored in accordingly when calculating partition sums. The computation of the state-dependent degeneracy factors can be found in Refs. [35,6].

The state-independent degeneracy factors occur in species where there are atoms that are not interchanged upon rotation. This degeneracy factor is expressed as $\prod (2I + 1)$, where I is the nuclear spin and

the product is taken over all nuclei not interchanged by rotation [35]. Often in the literature, the state-independent degeneracy factors are omitted from partition sum calculations when the application involves a ratio of partition sums. This applies to the partition functions of Sauval and Tatum [24], Irwin [25] and Barklem and Collet [28]. However, when determining thermodynamic quantities from the partition sum and its moment, the state-independent degeneracy factors must be included. In this work, all state-independent degeneracy factors were included, which is also the convention used by ExoMol.

The calculation of the internal partition sum, Eq. (2), requires a knowledge of the term values or energies and the corresponding degeneracy factors for the molecule/isotopologue in question. Eq. (2) suggests that as the energy increases, the exponential factor approaches zero and the sum can be truncated with no loss of accuracy. The energy at which the summation can be truncated depends on temperature, since kT divides the energy of the state. There are several methods that have been used to determine this cutoff, see Furtenbacher et al. [36] or Gamache et al. [7,33] for examples. This topic is discussed more below.

There are various ways to compute $Q(T)$ and the resulting accuracy depends on the inventory of energy states available for the molecule/isotopologue in question. Certainly, the best method is direct summation of Eq. (2), which requires term values up to 30 to 50 thousand cm^{-1} , depending on the highest temperature at which $Q(T)$ is computed. Modern *ab initio* calculations (see <https://www.exomol.com> [37] or <http://theorets.tsu.ru/molecules> [38] for examples) or *ab initio* calculations mixed with measured term values [36,39–45] are capable of providing such data sets for accurate computation of $Q(T)$ and thermodynamic functions to temperatures to 5000–9000 K. However, such term value data sets are not yet available for many of the molecules/isotopologues for which TIPS data are needed. Thus, approximations to the direct sum in Eq. (2) must be made.

The first step is usually to assume the motions (electronic, vibrational, rotational, torsional, Λ -doubling, etc.) are not coupled leading to the energies being additive

$$E_{elec, vib, rot, tors, \dots} = E_{elec} + E_{vib} + E_{rot} + E_{tors} + \dots \quad (3)$$

from which follows the product approximation

$$Q_{elec, vib, rot, tors, \dots} = Q_{elec} \times Q_{vib} \times Q_{rot} \times Q_{tors} \times \dots \quad (4)$$

Considering the cases where $Q_{elec}=1$ and Q_{tors} and other motions do not apply, the TIPS is the product of Q_{vib} and Q_{rot} . Q_{vib} is generally determined using the harmonic oscillator approximation [35] (HOA) and sometimes with anharmonic corrections [35]. If a full set of term values is available for the ground vibrational state, these can be used to determine Q_{rot} by direct summation, if not analytical approximations are used to determine Q_{rot} [46–49]. For details see Refs [3,4,6,7,50].

The cutoff in temperature that has been chosen (see Table 1) for each isotopologue is based on the particular term values available for each isotopologue. General guidelines were presented in Tables 2 and 3 of Gamache et al. [18] and are dependent on the spacing of the energy states of the molecule. The more tightly packed the energy states, the lower the cutoff temperature for a given F'_{max} . When the partition sums are determined via analytical formulas, the uncertainty is generally higher but the formulas are more appropriate for higher temperatures. Thus, in a number of cases the partition sums in TIPS2024 are a combination of direct sum results for the lower temperatures and analytical formula results for higher temperatures. The cross-over temperatures are determined separately for each isotopologue using the percent difference between DS (direct summation) and PA (product approximation) results. Because the scientific community often needs Q values at high temperatures, the cutoff temperatures in Table 1 are somewhat optimistic. It should be kept in mind that at the higher temperatures the uncertainty in Q will be greater than at the lower temperatures. In addition to listing the isotopologue formula, Table 1 also provides the Air Force Geophysics Laboratory (AFGL) code that was used in early

Table 1

Molecule number, chemical formula, isotopologue number (ISO#), AFGL code, state independent degeneracy factor (g_i), $Q(296\text{ K})$, and T_{max} in K.

Molecule #	Formula	ISO#	AFGL code	g_i	$Q(296\text{ K})$	T_{max} K
1	H_2^{16}O	1	161	1	1.7458×10^2	5000
	H_2^{18}O	2	181	1	1.7605×10^2	5000
	H_2^{17}O	3	171	6	1.0521×10^3	5000
	HD^{16}O	4	162	6	8.6474×10^2	5000
	HD^{18}O	5	182	6	8.7557×10^2	5000
	HD^{17}O	6	172	36	5.2268×10^3	5000
	D_2^{16}O	7	262	1	1.0278×10^3	6000
	D_2^{18}O	8	282	1	1.0434×10^3	6000
	D_2^{17}O	9	272	6	6.2160×10^3	6000
2	$^{12}\text{C}^{16}\text{O}_2$	1	626	1	2.8609×10^2	5000
	$^{13}\text{C}^{16}\text{O}_2$	2	636	2	5.7664×10^2	5000
	$^{16}\text{O}^{12}\text{C}^{18}\text{O}$	3	628	1	6.0781×10^2	3500
	$^{16}\text{O}^{12}\text{C}^{17}\text{O}$	4	627	6	3.5426×10^3	3500
	$^{16}\text{O}^{13}\text{C}^{18}\text{O}$	5	638	2	1.2255×10^3	3500
	$^{16}\text{O}^{13}\text{C}^{17}\text{O}$	6	637	12	7.1413×10^3	3500
	$^{12}\text{C}^{18}\text{O}_2$	7	828	1	3.2342×10^2	5000
	$^{17}\text{O}^{12}\text{C}^{18}\text{O}$	8	827	6	3.7666×10^3	3500
	$^{12}\text{C}^{17}\text{O}_2$	9	727	1	1.0972×10^4	5000
	$^{13}\text{C}^{18}\text{O}_2$	0	838	2	6.5224×10^2	5000
	$^{18}\text{O}^{13}\text{C}^{17}\text{O}$	11	837	12	7.5950×10^3	3500
	$^{13}\text{C}^{17}\text{O}_2$	12	737	2	2.2120×10^4	5000
	$^{14}\text{C}^{16}\text{O}_2$	13	646	1	2.9048×10^2	5000
	3	$^{16}\text{O}_3$	1	666	1	3.4750×10^3
$^{16}\text{O}^{16}\text{O}^{18}\text{O}$		2	668	1	7.5846×10^3	1000
$^{16}\text{O}^{18}\text{O}^{16}\text{O}$		3	686	1	3.7030×10^3	1000
$^{16}\text{O}^{16}\text{O}^{17}\text{O}$		4	667	6	4.4044×10^4	1000
$^{16}\text{O}^{17}\text{O}^{16}\text{O}$		5	676	6	2.1742×10^4	1000
$^{16}\text{O}^{18}\text{O}^{18}\text{O}$		6	688	1	7.9376×10^3	1000
$^{18}\text{O}^{16}\text{O}^{18}\text{O}$		7	868	1	4.0703×10^3	1000
$^{16}\text{O}^{17}\text{O}^{18}\text{O}$		8	678	6	4.6563×10^4	1000
$^{18}\text{O}^{16}\text{O}^{17}\text{O}$		9	867	6	4.7135×10^4	1000
$^{16}\text{O}^{18}\text{O}^{17}\text{O}$		10	687	6	4.6074×10^4	1000
$^{16}\text{O}^{17}\text{O}^{17}\text{O}$		11	677	36	2.7051×10^5	1000
$^{17}\text{O}^{16}\text{O}^{17}\text{O}$		12	767	1	1.3704×10^5	1000
$^{18}\text{O}_3$		13	888	1	4.2647×10^3	1000
$^{18}\text{O}^{18}\text{O}^{17}\text{O}$		14	887	6	4.9325×10^4	1000

(continued on next page)

Table 1 (continued)

Molecule #	Formula	ISO#	AFGL code	g_i	$Q(296\text{ K})$	T_{\max} K
	$^{18}\text{O}^{17}\text{O}^{18}\text{O}$	15	878	6	2.5005×10^4	1000
	$^{18}\text{O}^{17}\text{O}^{17}\text{O}$	16	877	36	2.8147×10^5	1000
	$^{17}\text{O}^{18}\text{O}^{17}\text{O}$	17	787	1	1.4342×10^5	1000
	$^{17}\text{O}_3$	18	777	6	8.4189×10^5	1000
4	$^{14}\text{N}_2^{16}\text{O}$	1	446	9	4.9850×10^3	5000
	$^{14}\text{N}^{15}\text{N}^{16}\text{O}$	2	456	6	3.3507×10^3	5000
	$^{15}\text{N}^{14}\text{N}^{16}\text{O}$	3	546	6	3.4472×10^3	5000
	$^{14}\text{N}_2^{18}\text{O}$	4	448	9	5.2969×10^3	5000
	$^{14}\text{N}_2^{17}\text{O}$	5	447	54	3.0868×10^4	5000
5	$^{12}\text{C}^{16}\text{O}$	1	26	1	1.0742×10^2	9000
	$^{13}\text{C}^{16}\text{O}$	2	36	2	2.2470×10^2	9000
	$^{12}\text{C}^{18}\text{O}$	3	28	1	1.1278×10^2	9000
	$^{12}\text{C}^{17}\text{O}$	4	27	6	6.6118×10^2	9000
	$^{13}\text{C}^{18}\text{O}$	5	38	2	2.3644×10^2	9000
	$^{13}\text{C}^{17}\text{O}$	6	37	12	1.3847×10^3	9000
	$^{14}\text{C}^{16}\text{O}$	7	46	1	1.1693×10^2	9000
	$^{14}\text{C}^{18}\text{O}$	8	48	1	1.2331×10^2	9000
	$^{14}\text{C}^{17}\text{O}$	9	47	6	7.2138×10^2	9000
6	$^{12}\text{CH}_4$	1	211	1	5.9053×10^2	2500
	$^{13}\text{CH}_4$	2	311	2	1.1811×10^3	2500
	$^{12}\text{CH}_3\text{D}$	3	212	3	4.7947×10^3	2500
	$^{13}\text{CH}_3\text{D}$	4	312	6	9.6010×10^3	2500
7	$^{16}\text{O}_2$	1	66	1	2.1573×10^2	7500
	$^{16}\text{O}^{18}\text{O}$	2	68	1	4.5523×10^2	7500
	$^{16}\text{O}^{17}\text{O}$	3	67	1	2.6581×10^3	7500
	$^{18}\text{O}^{18}\text{O}$	4	88	1	2.4232×10^2	7500
	$^{18}\text{O}^{17}\text{O}$	5	87	1	2.8191×10^3	7500
	$^{17}\text{O}^{17}\text{O}$	6	77	1	8.2238×10^3	7500
8	$^{14}\text{N}^{16}\text{O}$	1	46	3	1.1411×10^3	9000
	$^{15}\text{N}^{16}\text{O}$	2	56	2	7.8831×10^2	9000
	$^{14}\text{N}^{18}\text{O}$	3	48	3	1.2028×10^3	9000
	$^{14}\text{N}^{17}\text{O}$	4	47	18	7.0381×10^3	9000
	$^{15}\text{N}^{18}\text{O}$	5	58	2	8.3265×10^2	9000
	$^{15}\text{N}^{17}\text{O}$	6	57	12	4.8673×10^3	9000
9	$^{32}\text{S}^{16}\text{O}_2$	1	626	1	6.3391×10^3	5000
	$^{34}\text{S}^{16}\text{O}_2$	2	646	1	6.3678×10^3	5000
	$^{33}\text{S}^{16}\text{O}_2$	3	636	4	2.5607×10^4	5000

Table 1 (continued)

Molecule #	Formula	ISO#	AFGL code	g_i	$Q(296\text{ K})$	T_{\max} K
	$^{16}\text{O}^{32}\text{S}^{18}\text{O}$	4	628	1	1.3681×10^4	5000
10	$^{14}\text{N}^{16}\text{O}_2$	1	646	3	1.3622×10^4	5000
	$^{15}\text{N}^{16}\text{O}_2$	2	656	2	9.3216×10^3	5000
	$^{16}\text{O}^{14}\text{N}^{18}\text{O}$	3	648	3	1.4546×10^4	5000
11	$^{14}\text{NH}_3$	1	4111	3	1.7252×10^3	5000
	$^{15}\text{NH}_3$	2	5111	2	1.1533×10^3	5000
	$^{14}\text{NH}_2\text{D}$	3	4112	9	1.1431×10^4	5000
12	$\text{H}^{14}\text{N}^{16}\text{O}_3$	1	146	6	2.1393×10^5	3500
	$\text{H}^{15}\text{N}^{16}\text{O}_3$	2	156	4	1.4313×10^5	3500
13	^{16}OH	1	61	2	8.0348×10^1	9000
	^{18}OH	2	81	2	8.0881×10^1	5000
	^{16}OD	3	62	3	2.0931×10^2	5000
14	H^{19}F	1	19	4	4.1469×10^1	6000
	D^{19}F	2	29	6	1.1591×10^2	6000
15	H^{35}Cl	1	15	8	1.6065×10^2	6000
	H^{37}Cl	2	17	8	1.6089×10^2	6000
	D^{35}Cl	3	25	12	4.6278×10^2	6000
	D^{37}Cl	4	27	12	4.6413×10^2	6000
16	H^{79}Br	1	19	8	2.0017×10^2	6000
	H^{81}Br	2	11	8	2.0024×10^2	6000
	D^{79}Br	3	29	12	5.8640×10^2	6000
	D^{81}Br	4	21	12	5.8676×10^2	6000
17	H^{127}I	1	17	12	3.8899×10^2	6000
	D^{127}I	2	27	18	1.1471×10^3	6000
18	$^{35}\text{Cl}^{16}\text{O}$	1	56	4	3.2918×10^3	5000
	$^{37}\text{Cl}^{16}\text{O}$	2	76	4	3.3492×10^3	5000
19	$^{16}\text{O}^{12}\text{C}^{32}\text{S}$	1	622	1	1.2164×10^3	5000
	$^{16}\text{O}^{12}\text{C}^{34}\text{S}$	2	624	1	1.2488×10^3	5000
	$^{16}\text{O}^{13}\text{C}^{32}\text{S}$	3	632	2	2.4746×10^3	5000
	$^{16}\text{O}^{12}\text{C}^{33}\text{S}$	4	623	4	4.9313×10^3	5000
	$^{18}\text{O}^{12}\text{C}^{32}\text{S}$	5	822	1	1.3048×10^3	5000
	$^{16}\text{O}^{13}\text{C}^{34}\text{S}$	6	634	2	2.5416×10^3	5000
	$^{17}\text{O}^{12}\text{C}^{32}\text{S}$	7	722	6	7.5682×10^3	5000
20	$\text{H}_2^{12}\text{C}^{16}\text{O}$	1	126	1	2.8445×10^3	3500
	$\text{H}_2^{13}\text{C}^{16}\text{O}$	2	136	2	5.8368×10^3	5000
	$\text{H}_2^{12}\text{C}^{18}\text{O}$	3	128	1	2.9860×10^3	5000
21	$\text{H}^{16}\text{O}^{35}\text{Cl}$	1	165	8	1.9272×10^4	5000

(continued on next page)

Table 1 (continued)

Molecule #	Formula	ISO#	AFGL code	g_i	$Q(296\text{ K})$	T_{\max} K
22	$\text{H}^{16}\text{O}^{37}\text{Cl}$	2	167	8	1.9613×10^4	5000
	$^{14}\text{N}_2$	1	44	1	4.6710×10^2	9000
	$^{14}\text{N}^{15}\text{N}$	2	45	6	6.4410×10^2	9000
23	$^{15}\text{N}_2$	3	55	1	2.2230×10^2	9000
	$\text{H}^{12}\text{C}^{14}\text{N}$	1	124	6	8.9220×10^2	3500
	$\text{H}^{13}\text{C}^{14}\text{N}$	2	134	12	1.8310×10^3	3500
24	$\text{H}^{12}\text{C}^{15}\text{N}$	3	125	4	6.1528×10^2	3500
	$^{12}\text{CH}_3^{35}\text{Cl}$	1	215	4	5.7915×10^4	5000
	$^{12}\text{CH}_3^{37}\text{Cl}$	2	217	4	5.8832×10^4	5000
25	$\text{H}_2^{16}\text{O}_2$	1	1661	1	9.8480×10^3	6000
	$^{12}\text{C}_2\text{H}_2$	1	1221	1	4.1245×10^2	5000
	$\text{H}^{12}\text{C}^{13}\text{CH}$	2	1231	8	1.6557×10^3	5000
26	$\text{H}^{12}\text{C}^{12}\text{CD}$	3	1222	6	1.5937×10^3	5000
	$^{12}\text{C}_2\text{H}_6$	1	1221	1	7.0873×10^4	5000
	$^{12}\text{CH}_3^{13}\text{CH}_3$	2	1231	2	3.6183×10^4	5000
27	$\text{H}_3^{12}\text{C}_2\text{H}_2\text{D}$	3	1222	12	3.9266×10^5	5000
	$^{31}\text{PH}_3$	1	1111	2	3.2494×10^3	4500
	$^{12}\text{C}^{16}\text{O}^{19}\text{F}_2$	1	269	1	7.0028×10^4	3500
28	$^{13}\text{C}^{16}\text{O}^{19}\text{F}_2$	2	369	2	1.4006×10^5	3500
	$^{32}\text{S}^{19}\text{F}_6$	1	29	1	1.6110×10^6	5000
	H_2^{32}S	1	121	1	5.0579×10^2	4000
29	H_2^{34}S	2	141	1	5.0428×10^2	5000
	H_2^{33}S	3	131	4	2.0147×10^3	5000
	$\text{H}^{12}\text{C}^{16}\text{O}^{16}\text{OH}$	1	126	4	3.8860×10^4	5000
30	$\text{H}^{13}\text{C}^{16}\text{O}^{16}\text{OH}$	2	136	8	7.9038×10^4	5000
	H^{16}O_2	1	166	2	4.2998×10^3	5000
	$^{35}\text{Cl}^{16}\text{O}^{14}\text{N}^{16}\text{O}_2$	1	5646	12	4.7864×10^6	5000
31	$^{37}\text{Cl}^{16}\text{O}^{14}\text{N}^{16}\text{O}_2$	2	7646	12	4.9082×10^6	5000
	$^{14}\text{N}^{16}\text{O}^+$	1	46	3	3.1166×10^2	5000
	$\text{H}^{16}\text{O}^{79}\text{Br}$	1	169	8	2.8335×10^4	5000
32	$\text{H}^{16}\text{O}^{81}\text{Br}$	2	161	8	2.8233×10^4	5000
	$^{12}\text{C}_2\text{H}_4$	1	112,211	1	1.1042×10^4	5000
	$^{12}\text{CH}_2^{13}\text{CH}_2$	2	112,311	2	4.5231×10^4	5000
33	$^{12}\text{CH}_2^{13}\text{CHD}$	3	112,212	24	8.2452×10^4	5000
	$^{12}\text{CH}_3^{16}\text{OH}$	1	2161	1	7.0570×10^4	3500
	$^{12}\text{CH}_3^{79}\text{Br}$	1	219	4	8.3049×10^4	5000
34	$^{12}\text{CH}_3^{81}\text{Br}$	2	211	4	8.3392×10^4	5000

Table 1 (continued)

Molecule #	Formula	ISO#	AFGL code	g_i	$Q(296\text{ K})$	T_{\max} K
41	$^{12}\text{CH}_3^{12}\text{C}^{14}\text{N}$	1	2124	3	8.8659×10^4	5000
	$^{13}\text{CH}_3^{12}\text{C}^{14}\text{N}$	2	3124	6	1.8363×10^5	5000
	$^{12}\text{CH}_3^{13}\text{C}^{14}\text{N}$	3	2134	6	1.8093×10^5	5000
42	$^{13}\text{CH}_3^{13}\text{C}^{14}\text{N}$	4	3134	12	3.7410×10^5	5000
	$^{12}\text{C}^{19}\text{F}_4$	1	29	1	1.2686×10^5	5000
	$^{12}\text{C}_4\text{H}_2$	1	2211	1	9.8215×10^3	5000
43	$\text{H}^{12}\text{C}_3^{14}\text{N}$	1	12,224	6	2.4711×10^4	5000
	$\text{H}^{12}\text{C}_3^{15}\text{N}$	2	12,225	4	1.7040×10^4	5000
	$\text{H}^{12}\text{C}^{12}\text{C}^{13}\text{C}^{14}\text{N}$	3	12,234	12	4.9897×10^4	5000
44	$\text{H}^{12}\text{C}^{13}\text{C}^{12}\text{C}^{14}\text{N}$	4	12,324	12	4.9728×10^4	5000
	$\text{H}^{13}\text{C}^{12}\text{C}^{12}\text{C}^{14}\text{N}$	5	13,224	4	5.1552×10^4	5000
	$\text{D}^{12}\text{C}^{12}\text{C}^{12}\text{C}^{14}\text{N}$	6	22,224	9	4.5928×10^4	5000
45	H_2	1	11	1	7.6712	6000
	HD	2	12	6	2.9874×10^1	6000
46	$^{12}\text{C}^{32}\text{S}$	1	22	1	2.5318×10^2	5000
	$^{12}\text{C}^{34}\text{S}$	2	24	1	2.5774×10^2	5000
	$^{13}\text{C}^{32}\text{S}$	3	32	2	5.3745×10^2	5000
47	$^{12}\text{C}^{33}\text{S}$	4	23	4	1.0229×10^3	5000
	$^{32}\text{S}^{16}\text{O}_3$	1	26	1	7.7833×10^3	3500
	$^{14}\text{N}^{12}\text{C}^{12}\text{C}^{14}\text{N}$	1	4224	1	1.5585×10^4	5000
48	$^{15}\text{N}^{12}\text{C}^{12}\text{C}^{15}\text{N}$	2	5225	1	7.3662×10^3	5000
	$^{12}\text{C}^{16}\text{O}^{35}\text{Cl}_2$	1	2655	1	1.4800×10^6	5000
	$^{12}\text{C}^{16}\text{O}^{35}\text{Cl}^{37}\text{Cl}$	2	2657	16	3.0435×10^6	5000
49	$^{32}\text{S}^{16}\text{O}$	1	26	1	8.4288×10^2	5000
	$^{34}\text{S}^{16}\text{O}$	2	46	1	8.5973×10^2	5000
	$^{32}\text{S}^{18}\text{O}$	3	28	1	9.1052×10^2	5000
50	$^{12}\text{CH}_3^9\text{F}$	1	219	2	1.4707×10^4	5000
	$^{13}\text{CH}_3^9\text{F}$	2	319	4	3.0239×10^4	5000
	$^{74}\text{GeH}_4$	1	7411	1	1.7149×10^3	5000
51	$^{72}\text{GeH}_4$	2	7211	1	1.7149×10^3	5000
	$^{70}\text{GeH}_4$	3	7011	1	1.7148×10^3	5000
	$^{73}\text{GeH}_4$	4	7311	10	1.7150×10^4	5000
52	$^{76}\text{GeH}_4$	5	7611	1	1.7153×10^3	5000
	$^{32}\text{S}^{12}\text{C}^{32}\text{S}$	1	222	1	1.3465×10^3	5000
	$^{32}\text{S}^{12}\text{C}^{34}\text{S}$	2	224	1	2.7848×10^3	5000
53	$^{32}\text{S}^{12}\text{C}^{33}\text{S}$	3	223	4	1.0958×10^4	5000
	$^{32}\text{S}^{13}\text{C}^{32}\text{S}$	4	232	2	2.7543×10^3	5000
	$^{12}\text{CH}_3^{27}\text{I}$	1	217	6	1.6427×10^5	5000

(continued on next page)

Table 1 (continued)

Molecule #	Formula	ISO#	AFGL code	g_i	$Q(296\text{ K})$	T_{\max} K
	$^{13}\text{CH}_3^{27}\text{I}$	2	317	12	3.4936×10^5	5000
55	$^{14}\text{N}^{19}\text{F}_3$	1	49	3	3.4773×10^5	5000
56	H_3^+	1	111	1	5.0355×10^1	5000
	H_2D^+	2	112	3	2.2485×10^2	2500
	HD_2^+	3	122	2	4.7790×10^2	4500
	D_3^+	4	222	1	3.4209×10^2	2500
57	$^{12}\text{CH}_3$	1	2111	1	6.6867×10^2	5000
58	$^{32}\text{S}_2$	1	22	1	1.0067×10^3	5000
59	$^{12}\text{C}^{16}\text{O}^{19}\text{F}^{35}\text{Cl}$	1	2695	8	6.2094×10^5	5000
	$^{12}\text{C}^{16}\text{O}^{19}\text{F}^{37}\text{Cl}$	2	2697	8	6.4040×10^5	5000
60	$\text{H}^{16}\text{O}^{14}\text{N}^{16}\text{O}$	1	1646	6	8.5076×10^4	5000
	$\text{H}^{16}\text{O}^{14}\text{N}^{16}\text{O}$	2	2646	9	1.4730×10^5	5000
61	$^{35}\text{Cl}^{14}\text{N}^{16}\text{O}_2$	1	5466	12	4.7838×10^5	5000
	$^{37}\text{Cl}^{14}\text{N}^{16}\text{O}_2$	2	7466	12	4.9380×10^5	5000
62	$^{12}\text{C}_3\text{H}_8$	1	1221	2	7.4879×10^4	5000

Table 2

Rotational partition sums for $^{14}\text{NH}_2\text{D}$ from Melosso et al. [60] compared with the calculations made here (TW).

T / K	$Q_{\text{Melosso et al.}}$	Q_{TW}	% difference
75.	1444.9034	1444.9081	0.0033
150.	4039.9313	4021.8131	0.45
225.	7398.7941	7362.3357	0.49
300.	11,379.1737	11,314.959	0.56

Table 3

OCS isotopologues, state-independent degeneracy factor, the maximum term values, and the cross-over temperatures that ensure convergence.

Isotopologue	g_{si}	F / cm^{-1}	$T_{\text{cross-over}} / \text{K}$
$^{16}\text{O}^{12}\text{C}^{32}\text{S}$	1	30,919.3425	3380
$^{16}\text{O}^{12}\text{C}^{34}\text{S}$	1	23,026.5752	3346
$^{16}\text{O}^{13}\text{C}^{32}\text{S}$	2	23,064.6129	3357
$^{16}\text{O}^{12}\text{C}^{33}\text{S}$	4	23,023.1799	762
$^{18}\text{O}^{12}\text{C}^{32}\text{S}$	1	23,054.0014	3567
$^{16}\text{O}^{13}\text{C}^{34}\text{S}$	2	23,026.5752	3235
$^{17}\text{O}^{12}\text{C}^{32}\text{S}$	6	23,037.7018	754

versions of HITRAN.

3. Calculations

Table 1 lists the molecules/isotopologues on HITRAN2024 and propane, which is not yet in the HITRAN database. Shown are the molecule number, isotopologue number, the original HITRAN isotopologue code, $Q(296\text{ K})$, and maximum temperature of the calculation. All of the molecules/isotopologues not mentioned below have been recalculated using the latest CODATA-recommended physical constants [34] and in some cases the temperature range extended (see Table 1). While the differences from using the updated constants are exceedingly small, the difference occurs at the sixth significant digit, TIPS2024

partition sums are all generated using the same constants. Below the calculations for the molecules/isotopologues are discussed in order of HITRAN molecule number.

3.1. Molecule 4, N_2O

Total internal partition sums were computed via direct summation for 12 isotopologues of N_2O ($^{14}\text{N}_2^{16}\text{O}$, $^{14}\text{N}^{15}\text{N}^{16}\text{O}$, $^{15}\text{N}^{14}\text{N}^{16}\text{O}$, $^{14}\text{N}_2^{18}\text{O}$, $^{14}\text{N}_2^{17}\text{O}$, $^{15}\text{N}_2^{16}\text{O}$, $^{15}\text{N}^{14}\text{N}^{18}\text{O}$, $^{15}\text{N}^{14}\text{N}^{17}\text{O}$, $^{14}\text{N}^{15}\text{N}^{18}\text{O}$, $^{14}\text{N}^{15}\text{N}^{17}\text{O}$, $^{15}\text{N}_2^{18}\text{O}$, $^{15}\text{N}_2^{17}\text{O}$) using the *ab initio* term values of Huang et al. [51]. The term values for the 5 most abundant isotopologues go up to $\sim 25\,000\text{ cm}^{-1}$, for $^{15}\text{N}_2^{16}\text{O}$ up to $\sim 19\,600\text{ cm}^{-1}$, and for the lesser six isotopologues up to $\sim 15\,000\text{ cm}^{-1}$. Only the 5 most abundant isotopologues (which are on HITRAN and labeled 446, 456, 546,448, and 447) are added to TIPS2024. For these isotopologues, the term values are not sufficient to give accurate results to 5000 K. To augment the data, the product approximation calculations, analytical Q_{rot} [46] and Q_{vib} by the harmonic oscillator approximation [35], done previously [7] were recalculated using the latest CODATA constants [34]. The DS and PA calculations were compared and the temperature where the percent difference becomes greater than 1 % was taken as the temperature to splice the DS and PA results. The cross-over temperatures are 4520, 3965, 3931, 3909, 3943 K, respectively. Fig. 1 shows the final TIPS for the 446, 456, 546,448 isotopologues. The direct sum data are plotted as a dashed blue line and the PA data as a red solid line. T_{\max} was set to 5000 K for each isotopologue. TIPS for the 7 lesser abundant isotopologues are available from the corresponding author.

3.2. Molecule 10, $^{16}\text{O}^{14}\text{N}^{18}\text{O}$ isotopologue

The $^{16}\text{O}^{14}\text{N}^{18}\text{O}$ isotopologue is an asymmetric rotor with C_1 symmetry. There are no similar atoms exchanged in symmetry operations so the state-independent degeneracy factor is $d_i = (2 I_{eO} + 1)(2 I_{4N} + 1)(2 I_{18O} + 1) = (2 * 0 + 1)(2 * 1 + 1)(2 * 0 + 1) = 3$. The calculation of the TIPS used the product approximation with Q_{vib} being calculated using the harmonic oscillator approximation [35] with $\nu_1 = 1306.692\text{ cm}^{-1}$, $\nu_2 = 745.54\text{ cm}^{-1}$, and $\nu_3 = 1659.44\text{ cm}^{-1}$ from Marinina et al. [52]. Q_{rot} was calculated using the analytical formula of Watson [49] with the rotational constants of Volkers et al. [53]. The calculations for Q_{vib} and Q_{rot} were made from 1 to 5000 K in 1 K steps. The Q_{vib} calculated here at 296 K, 1.029529, compares well with that from Marinina et al., however, Q_{rot} (296 K) from this work, 18,541.942, is roughly half that reported by Marinina et al., 28,270.764. A direct sum using their energies gives Q_{rot} (296 K) = 14,130.670; a factor of 2 less than what they reported. Their reported Q_{rot} values are also a factor of 2 too large. The analytical formula does not give reliable results for very low temperatures, so Q_{rot} values were calculated via direct sum using the term values from Marinina et al. and Q_{vib} calculated using the harmonic oscillator approximation. These data were compared with the product approximation calculations and the cross-over temperature was taken when the percent difference is greater than 1.

For the 2 most abundant isotopologues of NO_2 , $^{14}\text{N}^{16}\text{O}_2$ and $^{15}\text{N}^{16}\text{O}_2$, a similar procedure was used. First, product approximation calculations were made using Watson's analytical formula [49] with the rotational constants of Bowman and De Lucia [54] for $^{14}\text{N}^{16}\text{O}_2$ and those of Perrin et al. [55] for $^{15}\text{N}^{16}\text{O}_2$ to calculate Q_{rot} . Q_{vib} was calculated using the harmonic oscillator approximation with vibrational term values from Norton and Rinsland [56] ($^{14}\text{N}^{16}\text{O}_2$) and from Perrin et al. [55] ($^{15}\text{N}^{16}\text{O}_2$). Next, Q_{rot} was calculated via direct summation using (000) state term values taken from the GEISA database [57]. The product approximation using DS Q_{rot} and analytical Q_{vib} and the values compared to the purely analytical PA. The final Q_{tot} values are the DS Q_{rot} and analytical Q_{vib} data at low temperatures and purely analytical PA at high temperatures. The cross-over temperature was taken when the two methods of calculations differ by $>1\%$. Fig. 2 shows Q_{tot} from DS Q_{rot} and analytical Q_{vib} (blue dashed line) and Q_{tot} from the purely

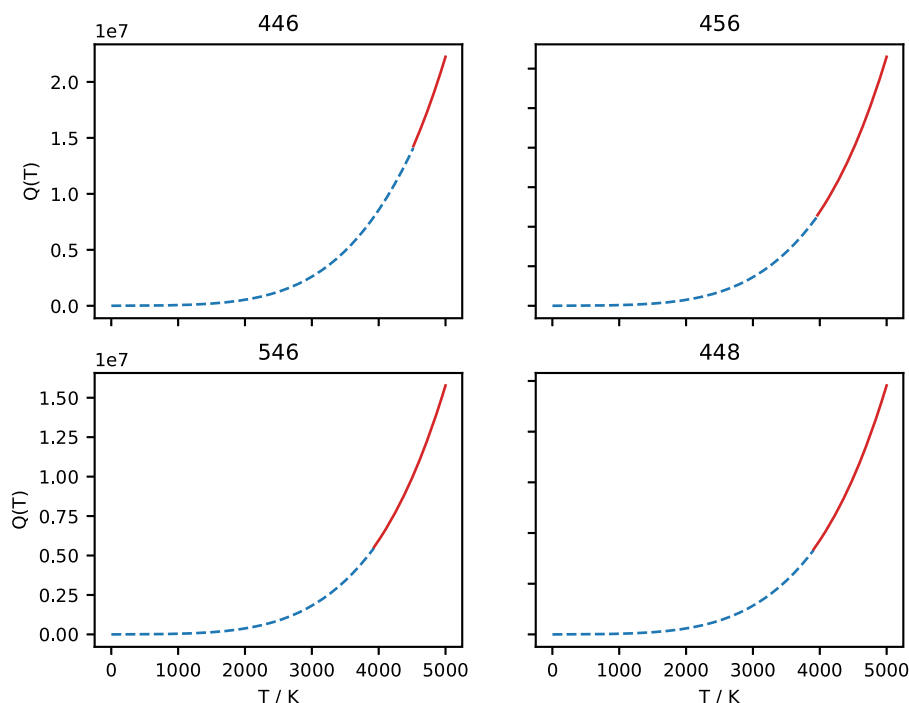


Fig. 1. TIPS for the 446, 456, 546, and 448 isotopologues of N_2O versus temperature. Values calculated by direct summation are the dashed blue line and those determined via the product approximation are the red solid line.

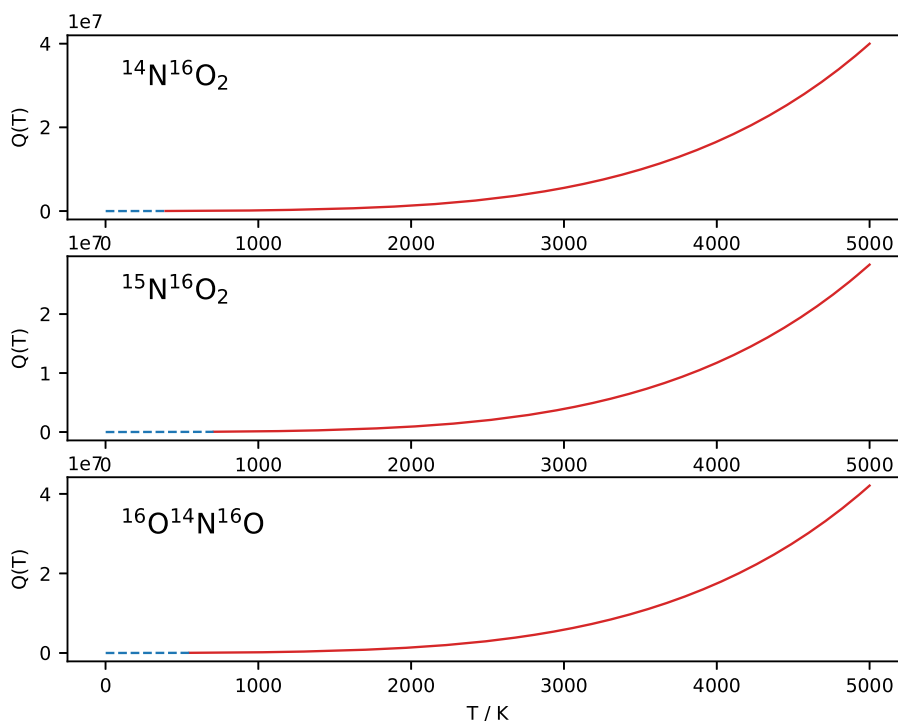


Fig. 2. Final Q_{tot} from DS Q_{rot} and analytical Q_{vib} (blue dashed line) and Q_{tot} from the purely analytical PA (red solid line) versus temperature for $^{14}\text{N}^{16}\text{O}_2$ (top panel), $^{15}\text{N}^{16}\text{O}_2$ (middle panel), and $^{16}\text{O}^{14}\text{N}^{16}\text{O}$ (bottom panel).

analytical PA (red solid line) versus temperature for $^{14}\text{N}^{16}\text{O}_2$, $^{15}\text{N}^{16}\text{O}_2$, and $^{16}\text{O}^{14}\text{N}^{16}\text{O}$. The cross-over temperatures are 393, 708, and 550 K, respectively. The final TIPS are reported from 1 to 5000 K in 1 K steps.

3.3. Molecule 11, $^{14}\text{NH}_2\text{D}$ isotopologue

The $^{14}\text{NH}_2\text{D}$ isotopologue of ammonia is an asymmetric rotor with C_s

symmetry. The H atoms are exchanged in symmetry rotations giving a state-dependent degeneracy factor of 3 for odd states and 1 for even states. In addition, the state-independent degeneracy factor is $(2I_{z_N} + 1)(2I_{z_H} + 1) = 9$. The product approximation was used to determine the TIPS. Q_{vib} was calculated using the harmonic oscillator approximation [35] (HOA) with the vibrational frequencies reported by Snels et al. [58]. The analytical formula of Watson was used to determine Q_{rot} using

the ground vibrational state rotational constants of Canè et al. [59]. The calculations were made from 1 to 5000 K in 1 K steps. The resulting values at 296 K are 1.0308 and 11,088.4678, respectively. Melosso et al. [60] determined the term values for $^{14}\text{NH}_2\text{D}$ and calculated $Q_{\text{rot}}(T)$ for ortho and para states separately from 2.725 to 300 K. Table 2 shows their Q (ortho and para summed) compared with the calculations made here.

The two most abundant isotopologues of NH_3 were redone as follows. The TIPS determined using *ab initio* term values [7] were taken, $Q_{\text{DS}}(T)$. Calculations were made via the product approximation, where for $^{14}\text{NH}_3$ and $^{15}\text{NH}_3$, Q_{rot} values are calculated using the analytical expression of McDowell [47] with the constants of Poynter and Margolis [50] and Carlotti et al. [51], respectively. The vibrational partition sums are calculated in the HOA using the vibrational energies reported by Norton and Rinsland [56]. $Q_{\text{PA}}(T)$ were computed by the product approximation from 1 to 5000 K in 1 K steps. The state-independent statistical factors are 3 and 2 for $^{14}\text{NH}_3$ and $^{15}\text{NH}_3$, respectively. Next, the direct sum and product approximation data were compared. Fig. 3 shows Q_{DS} (blue dashed line) and Q_{PA} (red solid line) versus temperature for $^{14}\text{NH}_3$ in the top panel and $^{15}\text{NH}_3$ in the bottom panel. Using a 1 % difference as the cutoff, the cross-over temperatures are 692 and 947 K for $^{14}\text{NH}_3$ and $^{15}\text{NH}_3$, respectively. The difference in the cross-over temperatures coming from the $^{14}\text{NH}_3$ terms values being more extensive. The final TIPS are direct sums up to $T_{\text{cross-over}}-1$ and PA data from $T_{\text{cross-over}}$ to 5000 K.

3.4. Molecule 19, OCS

The TIPS for 7 isotopologues of carbonyl sulfide were considered: $^{16}\text{O}^{12}\text{C}^{32}\text{S}$, $^{16}\text{O}^{12}\text{C}^{34}\text{S}$, $^{16}\text{O}^{13}\text{C}^{32}\text{S}$, $^{16}\text{O}^{12}\text{C}^{33}\text{S}$, $^{18}\text{O}^{12}\text{C}^{32}\text{S}$, $^{16}\text{O}^{13}\text{C}^{34}\text{S}$, $^{17}\text{O}^{12}\text{C}^{32}\text{S}$. All except $^{17}\text{O}^{12}\text{C}^{32}\text{S}$ were considered in TIPS2020 [7]. However, there are now *ab initio* term values, F , available for the 7 isotopologues from Huang et al. [61]. These term values are not sufficient to converge Q to 5000 K (see Table 3 for maximum term values) so both direct summations using the *ab initio* term values and by the product approximation using Q_{rot} analytical times Q_{vib} harmonic oscillator approximation were done to determine $Q_{\text{DS}}(T)$ and $Q_{\text{PA}}(T)$. The direct sums were made using the term values of Huang et al. with the

state-independent degeneracy factors in Table 3. The product approximation calculations used the linear formula of McDowell [46] for Q_{rot} starting with the molecular constants used in Ref. [7]. These calculations gave $Q_{\text{PA}}(T)$ values for 3 isotopologues a few percent off from the direct sums. The rotational constants used were from measurements made in the seventies and eighties [62,63] and the vibrational fundamentals from Refs. [56,64,65] for the isotopologues in question are estimates. The vibrational data was updated using the data of Huang et al. [61]. To check the rotational constants, the rotation band data were taken from the data of Huang et al. for each isotopologue and were fit to the standard expression to determine B , D , and H . Using these new constants, $Q_{\text{DS}}(T)$ and $Q_{\text{PA}}(T)$ values now agree for all isotopologues at low temperatures. Fig. 4 shows Q_{DS} (blue dashed line) and Q_{PA} (red solid line) versus temperature for the 622, 624, 623, 632, 822, 634, 722 isotopologues of OCS. Using these DS and PA files, the final TIPS were formed by using Q_{DS} from 1 K to the temperature, $T_{\text{cross-over}}-1$, where the percent difference between Q_{DS} and Q_{PA} is $<1\%$, and the product approximation results from $T_{\text{cross-over}}$ to T_{max} . Table 3 lists the cross-over temperatures for each isotopologue. The TIPS are reported from 1–5000 K.

3.5. Molecule 32, $\text{H}^{13}\text{C}^{16}\text{O}^{16}\text{OH}$ isotopologue

A new isotopologue of formic acid was added to HITRAN2024, $\text{H}^{13}\text{C}^{16}\text{O}^{16}\text{OH}$. The state-independent degeneracy for this isotopologue is 8. The vibrational partition sum was calculated using the harmonic oscillator approximation with vibrational frequencies from Luiz et al. [66] for $\nu_1, \nu_2, \nu_3, \nu_4, \nu_5$ states, from Baskakov et al. [67] for the ν_6 and ν_8 states, and from Ong et al. [68] for the ν_7 and ν_9 states. The rotational partition sum was calculated using the analytical formula of Watson [49] with the rotational constants of Zhao et al. [69]. The calculations considered temperatures from 1 to 5000 K in 1 K steps.

3.6. Molecule 51, $^{13}\text{CH}_3^{19}\text{F}$ isotopologue

Like the principal isotopologue, $^{12}\text{CH}_3^{19}\text{F}$, $^{13}\text{CH}_3^{19}\text{F}$ is a symmetric rotor. The rotational partition sums were calculated using the analytical formula of McDowell [47], where the symmetry number is given by $\sigma =$

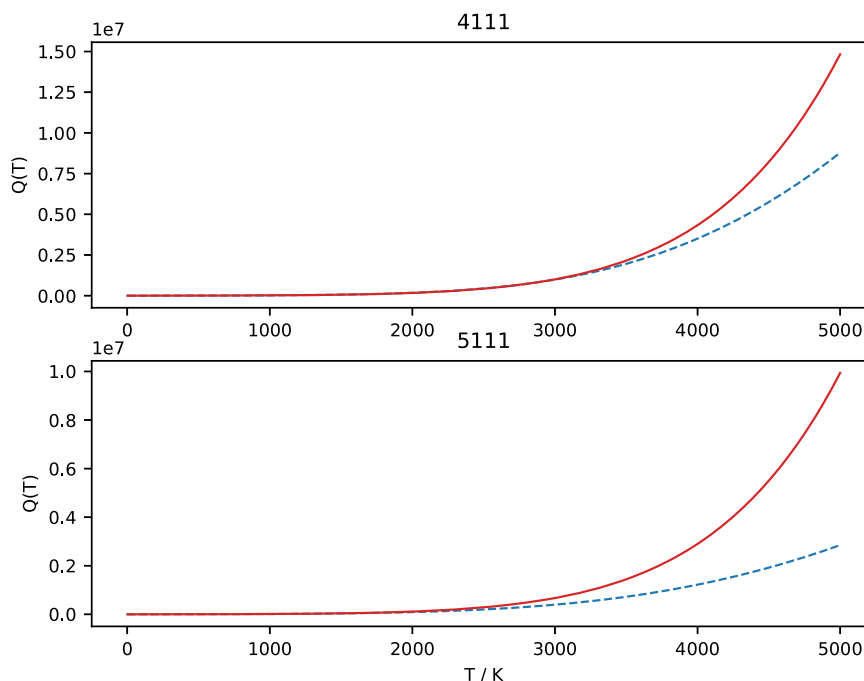


Fig. 3. TIPS determined using direct summation (blue dashed line) and product approximation (red solid line) versus temperature for $^{14}\text{NH}_3$ (top panel) and $^{15}\text{NH}_3$ (bottom panel).

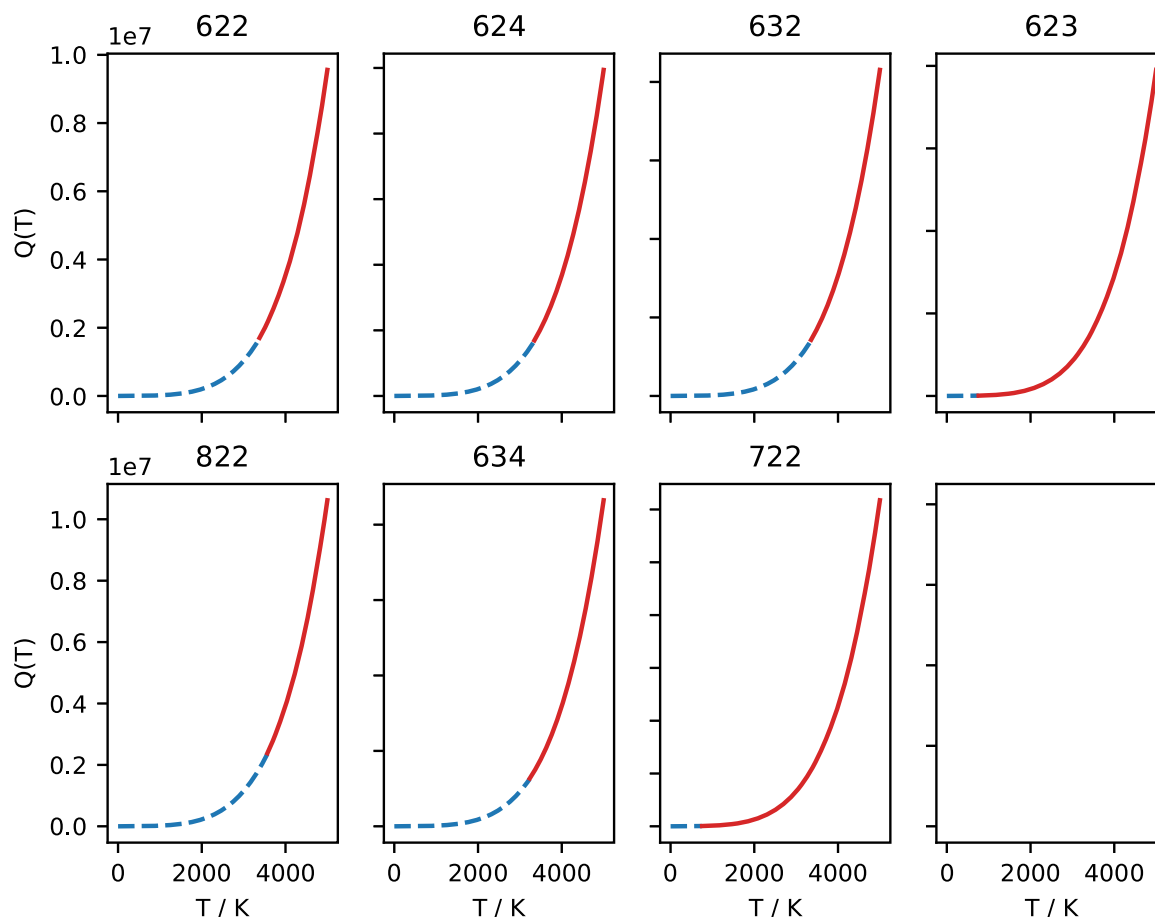


Fig. 4. Q_{DS} (blue dashed line) and Q_{PA} (red solid line) versus temperature for the 622, 624, 632, 623, 822, 634, 722 isotopologues of OCS as labeled.

$\frac{(2I+1)^3}{3}$, where I^* is the spin of the identical atoms being exchanged, here $I^*=1/2$, giving $\sigma=8/3$. The state-independent degeneracy factors are from ^{13}C and ^{19}F giving $d_i=4$. The rotational constants are from Papoušek et al. [70]. The vibrational partition sum was calculated via the harmonic oscillator approximation using the vibrational fundamentals, ν_1 through ν_6 , given in Papoušek et al. [70]. Q_{vib} and Q_{rot} were calculated from 1–5000 K in 1 K steps and the TIPS is given by their product.

3.7. Molecule 53, CS_2

The TIPS for 20 isotopologues of CS_2 were calculated using the *ab initio* term values of Huang et al. [71]. These calculated term values go up to 21 947 cm^{-1} (zero-point energy included) for the main isotopologue ($^{12}\text{C}^{32}\text{S}_2$), to $\sim 20,400$ cm^{-1} (zero-point energy included) for $^{12}\text{C}^{32}\text{S}_2$, $^{32}\text{S}^{12}\text{C}^{34}\text{S}$, $^{13}\text{C}^{32}\text{S}_2$, and $^{32}\text{S}^{12}\text{C}^{33}\text{S}$, to $\sim 13,800$ cm^{-1} (zero-point energy included) for $^{12}\text{C}^{33}\text{S}_2$ and $^{13}\text{C}^{33}\text{S}_2$, and to 15,363 cm^{-1} (zero-point energy included) for the other 13 minor isotopologues. Because of these cutoffs in the term values, the TIPS were determined by direct summation will only be converged to $\sim T=2500$ K. For the 4 isotopologues on HITRAN2020, $^{12}\text{C}^{32}\text{S}_2$, $^{32}\text{S}^{12}\text{C}^{34}\text{S}$, $^{13}\text{C}^{32}\text{S}_2$, $^{32}\text{S}^{12}\text{C}^{33}\text{S}$ (222, 224, 232, 223 in AFGL notation) the direct sum data were augmented using the product approximation. For $^{32}\text{S}^{12}\text{C}^{34}\text{S}$ and $^{32}\text{S}^{12}\text{C}^{33}\text{S}$, the rotational constants and vibrational fundamentals from Karlovets et al. [72] were used to compute $Q_{rot}(T)$ using the analytical expression of McDowell [46] and the $Q_{vib}(T)$ using the harmonic oscillator approximation of Herzberg [35]. However, because of the symmetry of $^{12}\text{C}^{32}\text{S}_2$ and $^{13}\text{C}^{32}\text{S}_2$, Bose systems (spin zero for the S atoms), the spin statistics complicates the determination of Q from the product approximation. For the symmetric Bose molecules, the triple product approximation (TPA)

must be done (see Gamache et al. [18] for details). The TIPS for the symmetric molecules were not correctly determined for TIPS2020 [7] and do not agree with the direct sums at low temperatures. To implement this procedure, the term values for both isotopologues were determined for $J=0$ to 200 (up to $\sim 20,450$ cm^{-1}) and the vibrational fundamentals from Karlovets et al. [72] were used to determine $Q(T)$ for both isotopologues via Eq. 28 of Gamache et al. [18]. Fig. 5 shows the direct sum partition sums (blue dashed line) and the PA (224 and 223) and TPA (222 and 232) partition sums (red solid line) for the 222, 224, 232, and 223 isotopologues. The temperature at which the DS and TPA results differ by $>1\%$, $T_{\text{cross-over}}$, is 2098 K, 571 K, 1182 K, and 561 K for the 222, 224, 232, and 223 isotopologues, respectively. The final TIPS are a cross-over of the DS results up to $T_{\text{cross-over}}-1$ and the product approximation results from $T_{\text{cross-over}}$ to T_{max} .

Table 4 presents for each isotopologue, the system label (Bose or Fermi), the direct sum partition sums at 296 K computed by Huang et al. [71] and those computed here, and the state-independent degeneracy factor. The agreement is excellent. When identical atoms that are interchanged by a symmetry operation have integer spin it is a Bose system or if they have half-integer spin it is a Fermi system. For the 323 and 333 isotopologues, where the ^{33}S atoms are interchanged in a 180° rotation, the state dependent degeneracy factors for even states have a weight of 6 and odd states have a weight of 10. The state independent degeneracy factors are 1 and 2, respectively. The 16 lesser isotopologues are not given in TIPS2024 but are available by contacting the corresponding author.

3.8. Molecule 56, H_3^+

The principal isotopologues of H_3^+ was added to HITRAN2024. Here

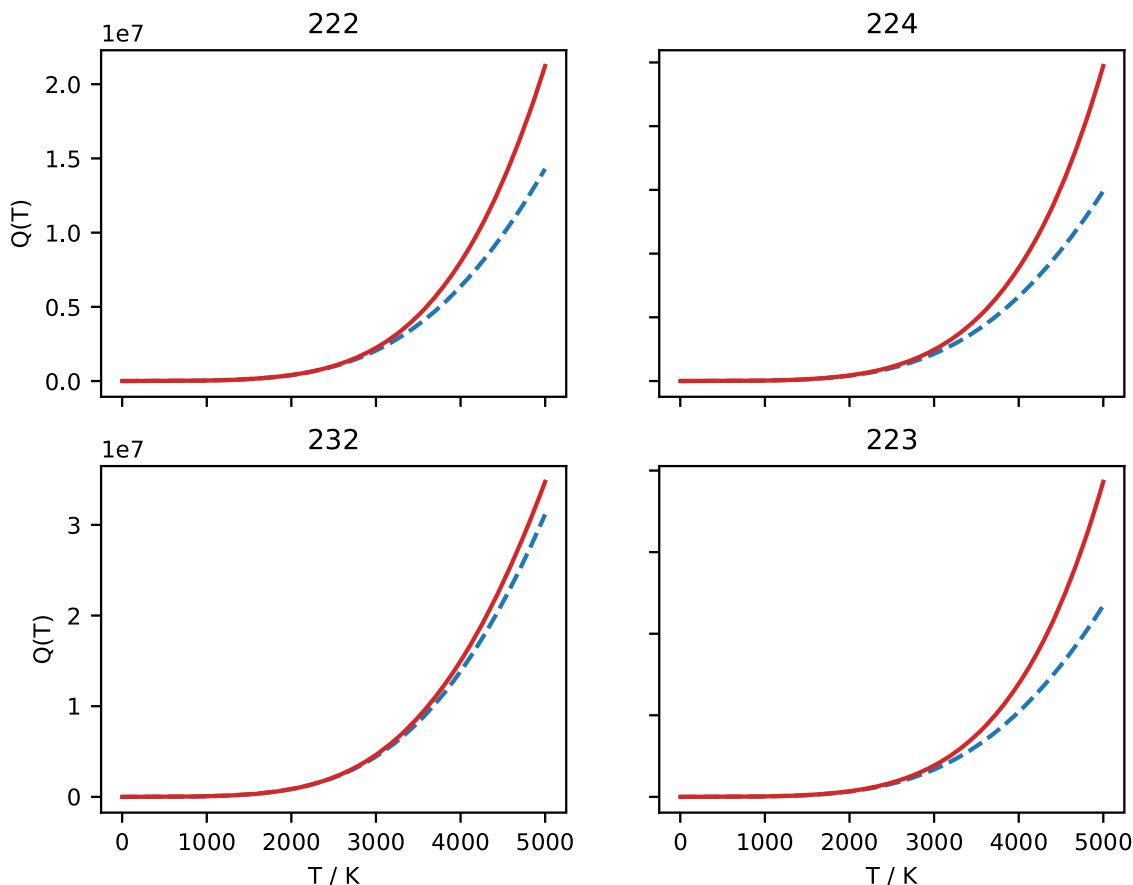


Fig. 5. Partition sums determined by direct summation (blue dashed line) and by the PA (red solid line) for 224 and 223 and TPA for the 222, 232 isotopologues of CS_2 versus temperature.

Table 4

Isotopologue number in AFGL notation, the system label when applicable (Bose or Fermi), the direct sum partition sums at 296 K computed by Huang et al. [71] and those computed here, and the state-independent degeneracy factor.

isotopologue	system	$Q_{\text{Huang et al.}}$	$Q_{\text{this work}}$	g_{si}
222	Bose	1346.52	1346.52	1
224		2784.78	2784.78	1
223		10,958.08	10,958.10	4
232	Bose	2754.32	2754.33	2
424	Bose	1440.91	1440.91	1
234		5697.86	5697.36	2
324		11,335.72	11,335.73	4
226		2872.44	2872.45	1
233		22,416.96	22,417.01	8
323	Fermi	22,298.72	22,299.29	1
434	Bose	2948.44	2948.44	2
426		2974.70	2974.70	1
334		23,193.60	23,193.62	8
236		5877.82	5877.82	2
326		11,695.44	11,695.44	4
333	Fermi	45,620.80	45,621.74	2
436		6087.96	6087.97	2
626	Bose	1536.35	1536.35	1
336	Fermi	23,936.80	23,936.83	8
636	Bose	3144.74	3144.75	2

we also calculate partition sums for H_2D^+ , HD_2^+ , and D_3^+ . The TIPS were calculated via a direct sum over the term values of Bowersman et al. [73], which uses the *ab initio* term values from Mizus et al. [74] along with empirical energy levels generated using the MARVEL procedure. This procedure produced term values for the isotopologues as shown in Table 5.

Table 5

Number of states, J_{max} , F_{max} and T_{max} for the isotopologues of H_3^+ .

Isotopologue	Number of states	J_{max}	$F_{\text{max}} \text{ cm}^{-1}$	$T_{\text{max}} / \text{K}$
H_3^+	158 721	37	42,001.	5000
H_2D^+	33 330	20	18,480.	2500
HD_2^+	369 501	25	34,779.	4500
D_3^+	37 410	15	17,140.	2500

Bowersman et al. [73] were able to assign quantum numbers to most states in their line list, whether empirical (MARVEL) or *ab initio*. Statistical weights were assigned to almost all states with $J \leq 20$ (term values to 25 000 cm^{-1}). In addition to the $2J+1$ statistical weight, each isotopologue has additional weights. For H_3^+ , the statistical weights for assigned states are equal to 2 for E states and 4 for A_2 states; states not assigned are given the average statistical weight of $8/3$. For H_2D^+ , the D atom gives a state independent weight of 3 and the state dependent factors are A_1 and A_2 states have $g_s=1$, B_1 and B_2 states have $g_s=3$. For the HD_2^+ isotopologue, H gives a state independent degeneracy factor of 2, and the state dependent factors are $g_s=6$ for A_1 and A_2 states and $g_s=3$ for B_1 and B_2 states. For D_3^+ , $g_s=10$ for A'_1 and A''_1 states, $g_s=1$ for A'_2 and A''_2 states, $g_s=4$ for E' and E'' states, $g_s=6$ for a_1 and a_2 states, $g_s=3$ for b_1 and b_2 states.

The calculations of the TIPS were made via direct summation at temperatures from 1 to the T_{max} (see Table 5) in 1 K steps. Comparing the TIPS for H_3^+ computed here with those of Bowersman et al. [73] shows large differences. Bowersman *et al.* note that they have followed the procedure of Neal and Tennyson [75], who state “All energies were taken relative to the $J = 0$ level of the vibrational ground state, which for H_3^+ has a statistical weight of zero.” Partition sums are over the existing

states of a molecule. The first occupied state of H_3^+ is $J = 1$ in the ground vibrational state at 64.121 cm^{-1} . Referencing the term values to a state that does not exist has the effect of scaling the TIPS; The use of a non-existent state with weight zero scales all other term values by an amount ΔE (here 64.121 cm^{-1}). Similar to the product approximation above, the two TIPS are related by $Q_{\text{this work}} = e^{hc \Delta E/k T} Q_{\text{ExoMol}}$. Fig. 6 demonstrates this scaling. Shown are the TIPS for H_3^+ , Q_{ExoMol} from Bowesman et al. [73] in blue solid circle symbols, the TIPS from scaling Q_{ExoMol} as the red solid line, and the TIPS computed here are the black solid circles. Table 6 shows the partition sums computed in this work and those from Bowesman et al. [73] for the other three isotopologues demonstrating excellent agreement.

3.9. Molecule 57, $^{12}\text{CH}_3$

While this molecule is new to HITRAN2024, it was considered in TIPS2020. Here the TIPS calculations were redone using the latest CODATA physical constants.

3.10. Molecule 58, $^{32}\text{S}_2$

The principal isotopologue of disulfur, $^{32}\text{S}_2$, was added to HITRAN2024. The total internal partition sum was calculated via direct summation. The term values are from the work of Gomez et al. [76] and include ro-vibrational term values for the ground electronic state, $X^3\Sigma_g^-$, the $a^1\Delta_g$, and the $b^1\Sigma_g^+$. The three electronic states have term values for $J = 0$ to 150 ($N = 1$ to 151). The ground electronic state considers ν from 0 to 10, and the term values go from 0 to $\sim 13,415 \text{ cm}^{-1}$. The first excited electronic state, $a^1\Delta_g$, considers ν from 0 to 21, and the term values go from 30,891 to $42,133 \text{ cm}^{-1}$, and the second excited electronic state, $b^1\Sigma_g^+$, considers ν from 0 to 21, and the term values go from 31690 to 45189 cm^{-1} . The TIPS were calculated via direct summation over the term values for temperatures from 1 to 5000 K in 1 K steps. The final TIPS agree with those of Gomez et al. (see Table 7), who report their data

Table 6

Partition sums for selected temperatures from the work of Bowesman et al. [73] and this work for the H_2D^+ , HD_2^+ , and D_3^+ isotopologues.

isotopologue	T / K	$Q_{\text{Bowesman et al.}}$	Q_{TW}
H_2D^+	296	224.86	224.849
	750	935.78	935.758
	1250	2408.7	2408.678
	2000	7463.9	7463.87
HD_2^+	296	477.8974	477.8974
	1250	5496.7042	5496.704
	3000	24,764.0	24,763.72
	5000	120,130.	120,130.7
	D_3^+	296	342.0941
	500	760.2250	760.22497
	600	1018.8229	1018.82289
	800	1676.1498	1676.14985

Table 7

Partition sums for $^{32}\text{S}_2$ from Gomez et al. [76] and this work (TW) at selected temperatures.

T / K	$Q_{\text{Gomez et al.}}$	Q_{TW}
60.	153.7423	153.7423
150.	462.9709	462.9707
220.	714.5863	714.5860
300.	1022.826	1022.825
500.	1945.129	1945.129
1000.	5416.679	5416.676
2000.	17,503.29	17,503.28
3000.	34,861.83	34,861.81
4000.	54,573.80	54,573.78

to seven significant figures on a 10 K grid from 1 to 4000 K.

3.11. Molecule 59, COFCl

There are two isotopologues of carbonic chloride fluoride,

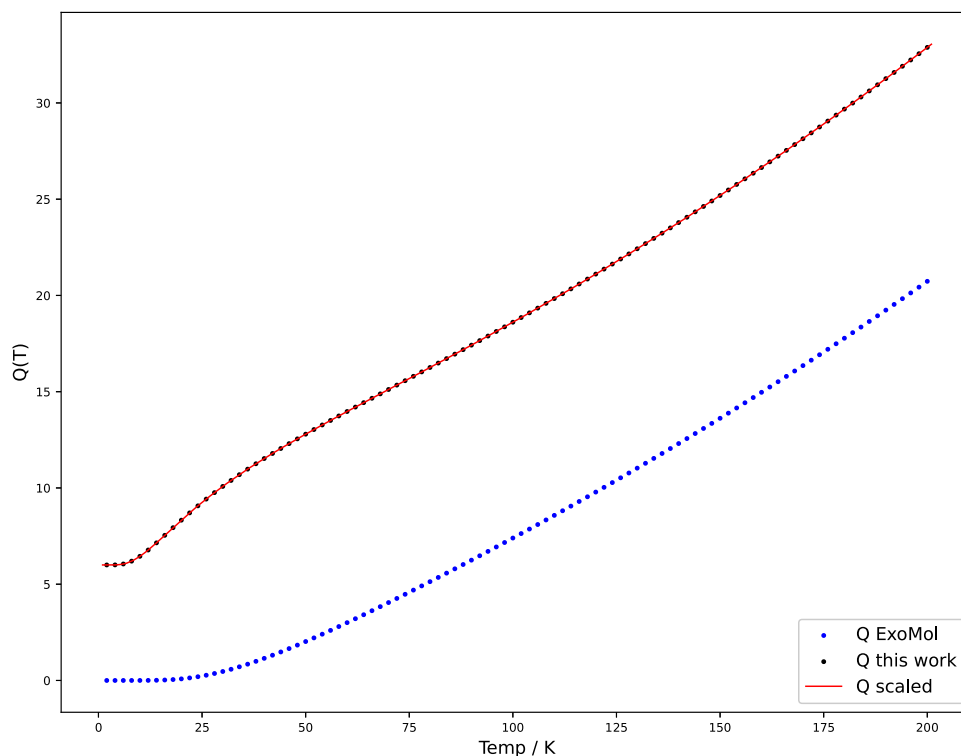


Fig. 6. The TIPS for H_3^+ : Q_{ExoMol} from Bowesman et al. [73] (blue solid circle symbols), the TIPS from scaling Q_{ExoMol} (red solid line), and the TIPS computed here (black solid circles) versus temperature.

$^{12}\text{C}^{16}\text{O}^{19}\text{F}^{35}\text{Cl}$ and $^{12}\text{C}^{16}\text{O}^{19}\text{F}^{37}\text{Cl}$, that are new to HITRAN2024. The AFGL isotopologue codes are 2695 and 2697, respectively. The TIPS were calculated using the product approximation from 1 to 5000 K in 1 K steps. The rotational partition sum was calculated via the analytical formula of Watson [49] with the rotational constants of Perrin et al. [77]. The state-independent degeneracy factor from the spins of the four atoms is 8 for both isotopologues. The vibrational partition sum was calculated via the harmonic oscillator approximation using fundamental frequencies from Perrin et al. [77,78]. The TIPS reported here at 296 K are 620,936.44 and 640,395.73 for the 2695 and 2697 isotopologues, respectively and agree well with those reported by Perrin et al. [77], 77, 145 and 77,869, respectively, when multiplied by the state-independent degeneracy factor.

3.12. Molecule 60, HONO

The TIPS for the two isotopologues of nitrous acid, $\text{H}^{16}\text{O}^{14}\text{N}^{16}\text{O}$ and $\text{D}^{16}\text{O}^{14}\text{N}^{16}\text{O}$, were calculated in this work (although only the principal isotopologue has been added to HITRAN2024) Both the cis- and trans-TIPS were computed and the total internal partition sum given by $Q_{\text{tot}}(T) = Q_{\text{vib,cis}}(T) * Q_{\text{rot,cis}}(T) + Q_{\text{vib,trans}}(T) * Q_{\text{rot,trans}}(T)$. The rotational constants are from Dehayem-Kamadjeu et al. [79]. The state-independent degeneracy factors coming from the spins of the four atoms are 6 and 9, respectively. The calculations for the vibrational partition sums used the harmonic oscillator approximation with vibrational frequencies from Refs. [79–87]. The calculations were made from 1 to 5000 K in 1 K steps. The calculations made here can be compared with the work of Sironneau et al. [80], which reported $Q_{\text{tot,cis}}(T)$ and $Q_{\text{tot,trans}}(T)$, and to the work of Tchana Betgna et al. [88], which reported $Q_{\text{tot}}(T)$, $Q_{\text{vib,cis}}(T)$, and $Q_{\text{vib,trans}}(T)$, and to the Jet Propulsion Lab (JPL) catalogue results [89], which reported $Q_{\text{tot}}(T)$. These data are presented in Table 8. There is very good agreement with the data of Tchana Betgna et al. and the JPL catalogue [89] at lower temperatures. It appears the JPL calculations do not have sufficient term values and become noticeably too low above 200 K. Sironneau et al. calculations for $Q_{\text{tot,cis}}(T)$ and $Q_{\text{tot,trans}}(T)$, are too similar to be correct. The ΔE between the cis and trans states is given as the vibrational ground state of the cis-isomer of HONO is higher in energy than the vibrational ground state of the trans-isomer of HONO by an amount $\Delta F_{\text{C-T}} = 99 \pm 25 \text{ cm}^{-1}$ [80]. Tchana Betgna et al. [88] give the cis-trans term value difference as $95.8 \pm 9.2 \text{ cm}^{-1}$, which was used in this work. Writing $Q_{\text{tot,cis}}(T)$ in terms of $Q_{\text{tot,trans}}(T)$ and the Term value difference gives

$$Q_{\text{tot,cis}}(T) = \sum_{\text{Cis states}} g e^{-(hc|F_{\text{Cis}} + \Delta F_{\text{C-T}})} = Q_{\text{tot,trans}}(T) * e^{-hc \Delta F_{\text{C-T}}/k T} \quad (5)$$

The factor $e^{-hc \Delta F_{\text{C-T}}/k T}$ is 0.618 at 296 K so taking their $Q_{\text{tot,trans}}$ gives a $Q_{\text{tot,cis}}$ equal to 32,015 at 296 K, in excellent agreement with the value determined here. For DONO Sironneau et al. give $\Delta F_{\text{C-T}} = 136 \pm 30 \text{ cm}^{-1}$ giving the factor 0.516 at 296 K. Using their $Q_{\text{tot,trans}}$ gives a $Q_{\text{tot,cis}}$ of 48,911, which is much closer to the value determined in this work. It appears that the factor $\Delta F_{\text{C-T}}$ was not included in their calculation.

Table 8

Partition sums for HONO isotopologues calculated in this work (TW) compared with the data of Sironneau et al. [80], Tchana Betgna et al. [88], and the JPL catalogue.

HONO Temp / K	Q_{tot} (Ref. [88])* g_i	Q_{tot} (TW)	Q_{tot} -JPL	$Q_{\text{vib-Cis}}$ (Ref. [88])	$Q_{\text{vib-Cis}}$ (TW)	$Q_{\text{vib-Trans}}$ (Ref. [88])	$Q_{\text{vib-Trans}}$ (TW)
75	6754.80	6695.697	6304.675	1.00004	1.000041	1.00001	1.000013
150	23,266.80	23,036.421	21,222.498	1.00931	1.009307	1.00537	1.005371
225	49,375.08	48,924.725	45,322.698	1.06240	1.062399	1.04296	1.042959
300	88,300.02	87,539.959	71,776.726	1.17490	1.174907	1.13050	1.130505
	$Q_{\text{tot-Cis}}$ (Ref. [80])* g_i	$Q_{\text{tot-Cis}}$ (TW)	$Q_{\text{tot-Trans}}$ (Ref. [80])* g_i	$Q_{\text{tot-Trans}}$ (TW)			
296	51,804	32,430.27	53,298	53,146.42			
DONO							
	$Q_{\text{tot-Cis}}$ (Ref. [80])* g_i	$Q_{\text{tot-Cis}}$ (TW)	$Q_{\text{tot-Trans}}$ (Ref. [80])* g_i	$Q_{\text{tot-Trans}}$ (TW)			
296	92,169	52,838.98	94,734	94,458.77			

3.13. Molecule 61, ClNO₂

There were two isotopologues of chlorine nitrite (IUPAC name chloro nitrite) added to HITRAN2024: $^{35}\text{Cl}^{14}\text{N}^{16}\text{O}_2$ and $^{37}\text{Cl}^{14}\text{N}^{16}\text{O}_2$. The TIPS were determined via the product approximation. Q_{vib} was computed using the harmonic oscillator approximation with the fundamental vibrational frequencies for both isotopologues use; ν_1 , ν_4 , ν_4 , and ν_6 from Shimanouchi et al. [90], ν_2 from Flaud et al. [91], and ν_3 from Anantharajah et al. [92]. Q_{rot} was calculated using the analytical formula of Watson with the rotational constants of Orphal et al. [93] for $^{35}\text{Cl}^{14}\text{N}^{16}\text{O}_2$ and the rotational constants of Flaud et al. [91] for $^{37}\text{Cl}^{14}\text{N}^{16}\text{O}_2$. The oxygen atoms are exchanged in 180° rotation, they are spin zero, this is a Bose system, i.e. half the states are missing. ^{35}Cl and ^{37}Cl are spin 3/2 and ^{14}N is spin 1 giving g_i equal to 12 for both isotopologues. The calculations were made from 1 to 5000 K in 1 K steps.

4. Codes to recall the TIPS

There are many applications that require the TIPS at various temperatures for a particular molecule and isotopologue. The HITRAN website (www.hitran.org) Supplemental/Total Internal Partition Sums/isotopologue metadata link gives a Table that lists the global ID, local ID, Formula, AFGL code, Abundance, Molar Mass/g mol⁻¹, $Q(296 \text{ K})$, $Q(\text{full range})$, and g_i . Under $Q(\text{full range})$ are links to the TIPS for the particular isotopologue for every reported temperature. While the data are there, the Table is not useful to researchers who need information for thousands of lines for numerous isotopologues and temperature. To aid researchers, codes have been developed to do this task [2,5–7,18]. Various methods have been used to recall $Q(T)$ in the past. Given the advancements in computers and storage, the FORTRAN code, TIPS2024_v1p0.FOR store the TIPS from 1–20 K in 1 K intervals and then from 22 K to T_{max} in 2 K steps for each isotopologue of each molecule shown in Table 1. This density of data allows linear interpolation to accurately determine $Q(T)$. Comparing the interpolated $Q(T)$ to the calculated values shows <0.001 absolute average percent difference. TIPS2024_v1p0.FOR is a stand-alone program that queries the user for molecule, isotopologue, and temperature and then returns $Q(T)$ for that species. TIPS2024_v1p0.FOR contains the subroutine BD_TIPS_2024 that users can insert into their codes to obtain $Q(T)$ for their applications. The algorithm recalls the TIPS by first checking if the requested temperature is one of the stored temperatures. If so, the TIPS value is returned, otherwise linear interpolation between the 2 points surrounding the requested temperature is done and that value returned. The state-independent degeneracy factor is also returned to allow comparison with other TIPS values in the literature.

Beginning in 2018 [6], a Python program has been provided for recalling the TIPS. In the first [6] and second [7] editions of the Python TIPS, Python libraries of the TIPS data were created for each isotopologue of each molecule and named by “molecule #”_“ISO#”.QTpy, where the molecule number and isotopologue number are given in Table 1. For example, the dictionary for the H_2^{18}O isotopologue of water (i.e. molecule 1, isotopologue 2) is 1_2.QTpy. In the 2024 edition,

TIPS2024_v1p0.py, the dictionaries are now dictionaries of dictionaries allowing a single dictionary for each molecule. These dictionaries contain the data for all isotopologues of the molecule and are labeled by the HITRAN molecule number. Examples for H₂O and CH₄ are 1.QTpy and 6.QTpy. The TIPS2024_v1p0.py code contains the def file (get_QT) that can be embedded in other Python codes to recall the TIPS. The method of recall is that of the FORTRAN codes.

The FORTRAN and Python codes and QT data are available as supplementary information, at ZENODO (zenodo.org/records/15,682,636), and at the HITRAN website (www.hitran.org). The Python libraries corresponding to TIPS2024/HITRAN2024 will also be incorporated into the HITRAN Application Programming Interface (HAPI) [94].

5. Summary

Total Internal Partition Sums (TIPS), $Q(T)$, were calculated for four new isotopologues of molecules on HITRAN2020 (¹⁶O¹⁴N¹⁸O, ¹⁴NH₂D, H¹³COOH, ¹³CH₃F), for the five most abundant isotopologues of N₂O, for the two most abundant isotopologues of NO₂, for the two most abundant isotopologues of NH₃, for the seven most abundant isotopologues of OCS, and for the four most abundant isotopologues of CS₂, and for six new molecules added to HITRAN2024: CH₃, S₂, COFCl (two isotopologues, ¹²C¹⁶O^{F35}Cl and ¹²C¹⁶O^{F37}Cl), HONO, ClNO₂ (two isotopologues, ³⁵ClNO₂ and ³⁷ClNO₂), and four isotopologues of H₃⁺: H₃⁺, H₂D⁺, HD₂⁺, and D₃⁺. The calculations for N₂ [32] and NO [33] were also added to TIPS2024 replacing the previous data. In addition, partition sums calculated prior to 2020 were recalculated using the most recent CODATA constants [34], while the differences are very small, TIPS2024 provides a consistent set of partition sums for all molecules/isotopologues on HITRAN2024. TIPS2024 also contains a number of isotopologues not on the HITRAN database. In total TIPS2024 provides data for 196 isotopologues of 62 molecules. The calculations range from $T = 1$ K to T_{\max} in 1 K steps. The maximum temperatures were determined based on the available energy states for the isotopologue in question and to ensure convergence of $Q(T)$. FORTRAN and Python algorithms to recall the TIPS as a function of molecule, isotopologue, and temperature are available for download (see above). Because of the density of the data, a simple linear interpolation routine provides values with <0.001 absolute average percent difference.

For the molecules/isotopologues that were present on TIPS2020, the changes in the partitions sums presented here will have a small impact on practical applications. However, this work will allow application codes to consider the six new molecules (eleven isotopologues) added to HITRAN2024 and thirty-three updated isotopologues. The improvement should be more noticeable at higher temperatures.

The FORTRAN and Python codes, and Table 1 are available in the supplementary information, at Zenodo (zenodo.org/records/15,682,636), and on the HITRAN website (www.hitran.org). Individual files of temperature and $Q(T)$ for each isotopologue studied are available from the corresponding author.

CRediT authorship contribution statement

Robert R. Gamache: Writing – review & editing, Writing – original draft, Validation, Software, Methodology, Formal analysis, Data curation, Conceptualization. **Bastien Vispoel:** Writing – review & editing, Writing – original draft, Validation, Software, Methodology, Formal analysis, Data curation. **Jonathan Tennyson:** Writing – review & editing, Writing – original draft, Data curation. **Sergei N. Yurchenko:** Writing – review & editing, Writing – original draft, Data curation. **Oleg L. Polyansky:** Writing – review & editing, Writing – original draft, Data curation. **Iouli E. Gordon:** Writing – review & editing, Writing – original draft, Methodology, Data curation. **Robert J. Hargreaves:** Writing – review & editing, Writing – original draft, Data curation. **Xinchuan Huang:** Writing – review & editing, Writing – original draft, Methodology, Data curation.

Declaration of competing interest

The authors declare that they have no known competing financial interests or personal relationships that could have appeared to influence the work reported in this paper.

Acknowledgments

B. Vispoel would like to thank the F.R.S.-FNRS for postdoctoral financial support. Work at UCL was supported by the European Research Council (ERC) under the European Union's Horizon 2020 research and innovation programme through Advance Grant number 883830. SY thanks the STFC Project No ST/Y001508/1. IEG and RJH are supported through NASA grant 80NSSC23K1596. XH acknowledges support from NASA/SETI Institute Cooperative Agreements 80NSSC19M0121 and 80NSSC20K1358.

Supplementary materials

Supplementary material associated with this article can be found, in the online version, at [doi:10.1016/j.jqsrt.2025.109568](https://doi.org/10.1016/j.jqsrt.2025.109568).

Data availability

Data and codes are available in supplementary information, on the HITRAN website, and on ZENODO.

References

- [1] Gamache RR, Hawkins RL, Rothman LS. Total internal partition sums in the temperature range 70-3000K: atmospheric linear molecules. *J Mol Spectrosc* 1990; 142:205–19.
- [2] Gamache RR, Kennedy S, Hawkins R, Rothman LS. Total internal partition sums for molecules in the terrestrial atmosphere. *J Mol Struct* 2000;517-518:413–31.
- [3] Fischer J, Gamache RR. Total internal partition sums for molecules of astrophysical interest. *J Quant Spectrosc Radiat Transf* 2002;74:263–72.
- [4] Fischer J, Gamache RR, Goldman A, Rothman LS, Perrin A. Total internal partition sums for molecular species on the 2000 edition of the HITRAN Database. *J Quant Spectrosc Radiat Transf* 2003;82:401–12.
- [5] Laraia AL, Gamache RR, Lamouroux J, Gordon IE, Rothman LS. Total internal partition sums to support planetary remote sensing. *Icarus* 2011;215:391–400.
- [6] Gamache RR, Roller C, Lopes E, Gordon IE, Rothman LS, Polyansky OL, Zobov NF, Kyuberis AA, Tennyson J, Yurchenko SN, Császár AG, Furtenbacher T, Huang X, Schwenke DW, Lee TJ, Drouin BJ, Tashkun SA, Perevalov VI, Kochanov RV. Total internal partition sums for 166 isotopologues of 51 molecules important in planetary atmospheres: application to HITRAN2016 and beyond. *J Quant Spectrosc Radiat Transf* 2017;203:70–87.
- [7] Gamache RR, Vispoel B, Rey M, Nikitin A, Tyuterev V, Egorov O, Gordon IE, Boudon V. Total internal partition sums for the HITRAN2020 database. *J Quant Spectrosc Radiat Transf* 2021;271:107713.
- [8] Rothman LS, Gamache RR, Goldman A, Brown LR, Toth RA, Pickett HM, Poynter RL, Flaud J-M, Camy-Peyret C, Barbe A, Husson N, Rinsland CP, Smith MAH. The HITRAN database: 1986 edition. *Appl Opt* 1987;26:4058–97.
- [9] Rothman LS, Gamache RR, Tipping RH, Rinsland CP, Smith MAH, Benner DC, Devi VM, Flaud J-M, Camy-Peyret C, Perrin A, Goldman A, Massie ST, Brown LR, Toth RA. The Hitran molecular database: editions of 1991 and 1992. *J Quant Spectrosc Radiat Transf* 1992;48:469–507.
- [10] Rothman LS, Rinsland CP, Goldman A, Massie ST, Edwards DP, Flaud J-M, Perrin A, Camy-Peyret C, Dana V, Mandin JY, Schroeder J, Mccann A, Gamache RR, Wattson RB, Yoshino K, Chance KV, Jucks KW, Brown LR, Nemtchinov V, Varanasi P. The Hitran molecular spectroscopic database and hawks(Hitran atmospheric workstation). *J Quant Spectrosc Radiat Transf* 1998;60: 665–710.
- [11] Rothman LS, Jacquemart D, Barbe A, Benner DC, Birk M, Brown LR, Carleer MR, Chackerian Jr C, Chance K, Coudert LH, Dana V, Devi VM, Flaud J-M, Gamache RR, Goldman A, Hartmann J-M, Jucks KW, Maki AG, Mandin J-Y, Massie ST, Orphal J, Perrin A, Rinsland CP, Smith MAH, Tennyson J, Tolchenov RN, Toth RA, Vander Auwera J, Varanasi P, Wagner G. The HITRAN 2004 molecular spectroscopic database. *J Quant Spectrosc Radiat Transf* 2005;96:139–204.
- [12] Rothman LS, Gordon IE, Barbe A, Benner DC, Bernath PF, Birk M, Boudon V, Brown LR, Campargue A, Champion JP, Chance K, Coudert LH, Dana V, Devi VM, Fally S, Flaud JM, Gamache RR, Goldman A, Jacquemart D, Kleiner I, Lacome N, Lafferty WJ, Mandin JY, Massie ST, Mikhailenko SN, Miller CE, Moazzen-Ahmadi N, Naumenko OV, Nikitin AV, Orphal J, Perevalov VI, Perrin A, Predoi-Cross A, Rinsland CP, Rotger M, Simečkova M, Smith MAH, Sung K, Tashkun SA, Tennyson J, Toth RA, Vandaele AC, Vander Auwera J. The HITRAN 2008

- molecular spectroscopic database. *J Quant Spectrosc Radiat Transf* 2009;110:533–72.
- [13] Rothman LS, Gordon IE, Babikov Y, Barbe A, Benner DC, Bernath PF, Birk M, Bizzocchi L, Boudon V, Brown LR, Campargue A, Chance K, Cohen EA, Coudert LH, Devi VM, Drouin BJ, Fayt A, Flaud JM, Gamache RR, Harrison JJ, Hartmann JM, Hill C, Hodges JT, Jacquemart D, Jolly A, Lamouroux J, Le Roy RJ, Li G, Long DA, Lyulin OM, Mackie CJ, Massie ST, Mikhailenko S, Müller HSP, Naumenko OV, Nikitin AV, Orphal J, Perevalov V, Perrin A, Polovtseva ER, Richard C, Smith MAH, Starikova E, Sung K, Tashkun S, Tennyson J, Toon GC, Tyuterev VG, Wagner G. The HITRAN2012 molecular spectroscopic database. *J Quant Spectrosc Radiat Transf* 2013;130:4–50.
- [14] Gordon IE, Rothman LS, Hill C, Kochanov RV, Tan Y, Bernath PF, Birk M, Boudon V, Campargue A, Chance KV, Drouin BJ, Flaud J-M, Gamache RR, Jacquemart D, Perevalov VI, Perrin A, Smith M-AH, Tennyson J, Tran H, Tyuterev VG, Toon GC, Hodges JT, Shine KP, Barbe A, Csaszar A, Devi MV, Furtenbacher T, Harrison JJ, Jolly A, Johnson T, Karman T, Kleiner I, Kyuberis A, Loos J, Lyulin O, Mikhailenko SN, Moazzen-Ahmadi N, Müller HSP, Naumenko O, Nikitin A, Polyansky O, Rey M, Rotger M, Sharpe S, Sung K, Starikova E, Tashkun SA, Auwera JV, Wagner G, Wilzewski J, Wcislo P, Yu S, Zak E. The HITRAN2016 molecular spectroscopic database. *J Quant Spectrosc Radiat Transf* 2017;203:3–69.
- [15] Gordon IE, Rothman LS, Hargreaves RJ, Hashemi R, Karlovets EV, Skinner FM, Conway EK, Hill C, Kochanov RV, Tan Y, Wcislo P, Finenko AA, Nelson K, Bernath PF, Birk M, Boudon V, Campargue A, Chance KV, Coustenis A, Drouin BJ, Flaud JM, Gamache RR, Hodges JT, Jacquemart D, Mlawer EJ, Nikitin AV, Perevalov VI, Rotger M, Tennyson J, Toon GC, Tran H, Tyuterev VG, Adkins EM, Baker A, Barbe A, Cané E, Császár AG, Dudaryonok A, Egorov O, Fleisher AJ, Fleurbaey H, Foltynowicz A, Furtenbacher T, Harrison JJ, Hartmann JM, Horneman VM, Huang X, Karman T, Karns J, Kassi S, Kleiner I, Kofman V, Kwabia-Tchana F, Lavrentieva NN, Lee TJ, Long DA, Lukashevskaya AA, Lyulin OM, Makhnev VY, Matt W, Massie ST, Melosso M, Mikhailenko SN, Mondelain D, Müller HSP, Naumenko OV, Perrin A, Polyansky OL, Raddaoui E, Raston PL, Reed ZD, Rey M, Richard C, Tóbiás R, Sadiek I, Schwenke DW, Starikova E, Sung K, Tamassia F, Tashkun SA, Vander Auwera J, Vasilenko IA, Viganin AA, Villanueva GL, Vispoel B, Wagner G, Yachmenev A, Yurchenko SN. The HITRAN2020 molecular spectroscopic database. *J Quant Spectrosc Radiat Transf* 2022;277:107949.
- [16] Edwards DP, López-Puertas M, Gamache RR. The non-LTE correction to the vibrational component of the internal partition sum for atmospheric calculations. *J Quant Spectrosc Radiat Transf* 1998;59:423–36.
- [17] Fischer J, Gamache RR. Partition sums for non-local thermodynamic equilibrium applications. *J Quant Spectrosc Radiat Transf* 2002;74:273–84.
- [18] Gamache RR, Vispoel B, Rey M, Tyuterev V, Barbe A, Nikitin A, Polyansky OL, Tennyson J, Yurchenko SN, Császár AG, Furtenbacher T, Perevalov VI, Tashkun SA. Partition sums for non-local thermodynamic equilibrium conditions for nine molecules of importance in planetary atmospheres. *Icarus* 2022;378: 114947 1:13.
- [19] Gamache RR, Goldman A. Einstein A coefficient, integrated band intensity, and population factors application to the $a^1\Delta_g-X^3\Sigma_g^-(0,0)$ O₂ band. *J Quant Spectrosc Radiat Transf* 2001;69:389–401.
- [20] Jacquinet-Husson N, Armande R, Scott NA, Chédin A, Crépeau L, Boutammine C, Bouhdaoui A, Crevoisier C, Capelle V, Boone C, Poulet-Crovisier N, Barbe A, Benner DC, Boudon V, Brown LR, Buldyreva J, Campargue A, Coudert LH, Devi VM, Down MJ, Drouin BJ, Fayt A, Fittschen C, Flaud JM, Gamache RR, Harrison JJ, Hill C, Hodnebrog Ø, Hu SM, Jacquemart D, Jolly A, Jiménez E, Lavrentieva NN, Liu AW, Lodi L, Lyulin OM, Massie ST, Mikhailenko S, Müller HSP, Naumenko OV, Nikitin A, Nielsen CJ, Orphal J, Perevalov VI, Perrin A, Polovtseva E, Predoi-Cross A, Rotger M, Ruth AA, Yu SS, Sung K, Tashkun SA, Tennyson J, Tyuterev VG, Vander Auwera J, Voronin BA, Makie A. The 2015 edition of the GEISA spectroscopic database. *J Mol Spectrosc* 2016;327:31–72.
- [21] Gamache RR, Vispoel B. On the temperature dependence of half-widths and line shifts for molecular transitions in the microwave and infrared regions. *J Quant Spectrosc Radiat Transf* 2018;217:440–52.
- [22] Smith MAH, Benner DC, Predoi-Cross A, Devi VM. Multispectrum analysis of ¹²CH₄ in the ν_4 band: I. Air-broadened halfwidths, pressure-induced shifts, temperature dependences and line mixing. *J Quant Spectrosc Radiat Transf* 2009;110:639–53.
- [23] Devi VM, Benner DC, Miller CE, Predoi-Cross A. Lorentz half-width, pressure-induced shift and speed-dependent coefficients in oxygen-broadened CO₂ bands at 6227 and 6348 cm⁻¹ using a constrained multispectrum analysis. *J Quant Spectrosc Radiat Transf* 2010;111:2355–69.
- [24] Sauval AJ, Tatum JB. A set of partition functions and equilibrium constants for 300 diatomic molecules of astrophysical interest. *Astrophys J Suppl Ser* 1984;56:193–209.
- [25] Irwin AW. Astronomy and astrophysics: refined diatomic partition functions I. Calculational methods and H₂ and CO results. *Astron Astrophys* 1987;182:348–58.
- [26] Irwin AW. The partition functions of JANAF polyatomic molecules that significantly affect the stellar atmospheric equations of state. *Astron Astrophys Suppl Ser* 1988;74:145–60.
- [27] Chase JMW, Davies CA, Downey JJR, Frurip DJ, McDonald RA, Syverud AN. JANAF thermochemical tables third edition. *J Phys Chem Ref Data* 1985;14 (Suppl.1):1–1856.
- [28] Barklem PS, Collet R. Partition functions and equilibrium constants for diatomic molecules and atoms of astrophysical interest. *A&A* 2016;588:A96.
- [29] Tennyson J, Yurchenko SN, Zhang J, Bowesman CA, Brady RP, Buldyreva J, Chubb KL, Gamache RR, Gorman MN, Guest ER, Hill C, Kefala K, Lynas-Gray AE, Mellor TM, McKemmish LK, Mitev GB, Mizus II, Owens A, Peng Z, Perri AN, Pezzella M, Polyansky OL, Qu Q, Semenov M, Smola O, Solokov A, Somogyi W, Upadhyay A, Wright SOM, Zobov NF. The 2024 release of the ExoMol database: molecular line lists for exoplanet and other hot atmospheres. *J Quant Spectrosc Radiat Transf* 2024;326:109083.
- [30] Fischer J, Gamache RR. Partition sums for non-local thermodynamic equilibrium applications. *J Quant Spectrosc Radiat Transf* 2002;74:273–84.
- [31] Rothman LS, Barbe A, Benner DC, Brown LR, Camy-Peyret C, Carleer MR, Chance K, Clerbaux C, Dana V, Devi VM, Fayt A, Flaud J-M, Gamache RR, Goldman A, Jacquemart D, Jucks KW, Lafferty WJ, Mandin J-Y, Massie ST, Nemtchinov V, Newnham DA, Perrin A, Rinsland CP, Schroeder J, Smith KM, Smith MAH, Tang K, Toth RA, Auwera JV, Varanasi P, Yoshino K. The HITRAN molecular spectroscopic database: edition of 2000 including updates through 2001. *J Quant Spectrosc Radiat Transf* 2003;82:5–44.
- [32] Gamache RR, Orphanos NG. Thermodynamic functions for N₂ from the total partition sum and its moments. *J Phys Chem Ref Data* 2023;52:023101.
- [33] Gamache RR, Orphanos NG, Qu Q, Yurchenko SN, Tennyson J. Ideal gas thermodynamic functions for NO from the total partition sum and its moments. *J Phys Chem Ref Data* 2024;53:033103.
- [34] Tiesinga E, Mohr PJ, Newell DB, Taylor BN. CODATA recommended values of the fundamental physical constants: 2018*. *J Phys Chem Ref Data* 2021;50:033105.
- [35] Herzberg G. Molecular spectra and molecular structure II. Infrared and Raman spectra of polyatomic molecules. New Jersey: D. Van Nostrand Company, Inc.; 1960.
- [36] Furtenbacher T, Horváth M, Koller D, Sólyom P, Balogh A, Balogh I, Császár AG. MARVEL analysis of the measured high-resolution rovibronic spectra and definitive ideal-gas thermochemistry of the ¹⁶O₂ molecule. *J Phys Chem Ref Data* 2019;48:023101.
- [37] Tennyson J, Yurchenko SN, Al-Refaie AF, Clark VJH, Chubb KL, Conway EK, Dewan A, Gorman MN, Hill C, Lynas-Gray AE, Mellor T, McKemmish LK, Owens A, Polyansky OL, Semenov M, Somogyi W, Tinetti G, Upadhyay A, Waldmann I, Wang Y, Wright S, Yurchenko OP. The 2020 release of the ExoMol database: molecular line lists for exoplanet and other hot atmospheres. *J Quant Spectrosc Radiat Transf* 2020;255:107228.
- [38] Rey M, Nikitin AV, Babikov YL, Tyuterev VG. TheoReTS – an information system for theoretical spectra based on variational predictions from molecular potential energy and dipole moment surfaces. *J Mol Spectrosc* 2016;327:138–58.
- [39] Furtenbacher T, Sziparovsky T, Hruby J, Kyuberis AA, Zobov NF, Polyansky OL, Tennyson J, Császár AG. Definitive ideal-gas thermochemical functions of the H₂¹⁶O molecule. *J Phys Chem Ref Data* 2016;45:043104.
- [40] Simkó I, Furtenbacher T, Hruby J, Zobov NF, Polyansky OL, Tennyson J, Gamache RR, Sziparovsky T, Dénes N, Császár AG. Recommended ideal-gas thermochemical functions for heavy water and its substituent isotopologues. *J Phys Chem Ref Data* 2017;46:023104.
- [41] Tennyson J, Bernath PF, Brown LR, Campargue A, Carleer MR, Császár AG, Gamache RR, Hodges JT, Jenouvrier A, Naumenko OV, Polyansky OL, Rothman LS, Toth RA, Vandaele AC, Zobov NF, Daumont L, Fazliev AZ, Furtenbacher T, Gordon IE, Mikhailenko SN, Shirin SV. IUPAC critical evaluation of the rotational–vibrational spectra of water vapor. Part I—Energy levels and transition wavenumbers for H₂¹⁷O and H₂¹⁸O. *J Quant Spectrosc Radiat Transf* 2009;110:573–96.
- [42] Tennyson J, Bernath PF, Brown LR, Campargue A, Császár AG, Daumont L, Gamache RR, Hodges JT, Naumenko OV, Polyansky OL, Rothman LS, Toth RA, Vandaele AC, Zobov NF, Fally S, Fazliev AZ, Furtenbacher T, Gordon IE, Hu S-M, Mikhailenko SN, Voronin BA. IUPAC critical evaluation of the rotational–vibrational spectra of water vapor. Part II: energy levels and transition wavenumbers for HD¹⁶O, HD¹⁷O, and HD¹⁸O. *J Quant Spectrosc Radiat Transf* 2010;111:2160–84.
- [43] Tennyson J, Bernath PF, Brown LR, Campargue A, Császár AG, Daumont L, Gamache RR, Hodges JT, Naumenko OV, Polyansky OL, Rothman LS, Vandaele AC, Zobov NF, Al Derzi AR, Fábri C, Fazliev AZ, Furtenbacher T, Gordon IE, Lodi L, Mizus II. IUPAC critical evaluation of the rotational–vibrational spectra of water vapor, Part III: energy levels and transition wavenumbers for H₂¹⁶O. *J Quant Spectrosc Radiat Transf* 2013;117:29–58.
- [44] Tennyson J, Bernath PF, Brown LR, Campargue A, Császár AG, Daumont L, Gamache RR, Hodges JT, Naumenko OV, Polyansky OL, Rothman LS, Vandaele AC, Zobov NF, Dénes N, Fazliev AZ, Furtenbacher T, Gordon IE, Hu S-M, Sziparovsky T, Vasilenko IA. IUPAC critical evaluation of the rotational–vibrational spectra of water vapor. Part IV. Energy levels and transition wavenumbers for D₂¹⁶O, D₂¹⁷O, and D₂¹⁸O. *J Quant Spectrosc Radiat Transf* 2014;142:93–108.
- [45] Tóbiás R, Furtenbacher T, Tennyson J, Császár AG. Accurate empirical rovibrational energies and transitions of H₂¹⁶O. *Phys Chem Chem Phys* 2019;21:3473–95.
- [46] McDowell RS. Rotational partition functions for linear molecules. *J Chem Phys* 1988;88:356–61.
- [47] McDowell RS. Rotational partition functions for symmetric-top molecules. *J Chem Phys* 1990;93:2801–11.
- [48] McDowell RS. Rotational partition functions for spherical-top molecules. *J Quant Spectrosc Radiat Transf* 1987;38:337–46.
- [49] Watson JKG. The asymptotic asymmetric-top rotational partition function. *Mol Phys* 1988;65:1377–97.
- [50] Goldman A, Gamache RR, Perrin A, Flaud J-M, Rinsland CP, Rothman LS. HITRAN partition functions and weighted transition probabilities. *J Quant Spectrosc Radiat Transf* 2000;66:455–86.
- [51] Huang X, Schwenke DW, Lee TJ. Highly accurate potential energy surface and dipole moment surface for nitrous oxide and 296K infrared line lists for ¹⁴N₂¹⁶O and

- minor isotopologues. *Mol Phys* 2024;122:e2232892. <https://doi.org/10.1080/00268976.2023.2232892>.
- [52] Marinina AA, Jacquemart D, Krim L, Soulard P, Perevalov VI. The ν_3 band of $^{16}\text{O}^{14}\text{N}^{18}\text{O}$: line positions and intensities. *J Quant Spectrosc Radiat Transf* 2022; 290:108312.
- [53] Volkers EA, Bulthuis J, Stolte S, Jost R, Linnartz H. High resolution electronic study of $^{16}\text{O}^{14}\text{N}^{16}\text{O}$, $^{16}\text{O}^{14}\text{N}^{18}\text{O}$ and $^{18}\text{O}^{14}\text{N}^{18}\text{O}$: a rovibronic survey covering 11800–14380 cm^{-1} . *J Mol Spectrosc* 2006;237:259–70.
- [54] Bowman WC, De Lucia FC. The millimeter and submillimeter spectrum of NO_2 : a study of electronic effects in a nonsinglet light asymmetric rotor. *J Chem Phys* 1982;77:92–107.
- [55] Perrin A, Toon G, Orphal J. Detection of atmospheric $^{15}\text{NO}_2$ in the ν_3 spectral region (6.3 μm). *J Quant Spectrosc Radiat Transf* 2015;154:91–7.
- [56] Norton RH, Rinsland CP. ATMOS data processing and science analysis methods. *Appl Opt* 1991;30:389–400.
- [57] Delahaye T, Armante R, Scott NA, Jacquinet-Husson N, Chédin A, Crépeau L, Crevoisier C, Douet V, Perrin A, Barbe A, Boudon V, Campargue A, Coudert LH, Ebert V, Flaud JM, Gamache RR, Jacquemart D, Jolly A, Kwabia Tchana F, Kyuberis A, Li G, Lyulin OM, Manceron L, Mikhailenko S, Moazzen-Ahmadi N, Müller HSP, Naumenko OV, Nikitin A, Perevalov VI, Richard C, Starikova E, Tashkun SA, Tyuterev VG, Vander Auwera J, Vispoel B, Yachmenev A, Yurchenko S. The 2020 edition of the GEISA spectroscopic database. *J Mol Spectrosc* 2021;380:111510.
- [58] Snels M, Hollenstein H, Quack M. The NH and ND stretching fundamentals of $^{14}\text{NH}_2\text{D}$. *J Mol Spectrosc* 2006;237:143–8.
- [59] Canè E, Di Lonardo G, Fusina L, Tamassia F, Predoi-Cross A. Mono- and di-deuterated ammonias: far-infrared spectra and spectroscopic parameters in the ground state. *J Mol Spectrosc* 2022;384:111581.
- [60] Melosso M, Bizocchi L, Dore L, Kisiel Z, Jiang N, Spezzano S, Caselli P, Gauss J, Pizzarrini C. Improved centrifugal and hyperfine analysis of ND_2H and NH_2D and its application to the spectral line survey of L1544. *J Mol Spectrosc* 2021;377: 111431.
- [61] Huang X, Gordon IE, Bertin T, Schwenke DW, Lee TJ. Accurate potential energy surface, dipole moment surface, and IR line lists for OCS isotopologues up to 2000 K. *J Quant Spectrosc Radiat Transf* 2025;339:109425.
- [62] Maki AG, Johnson DR. Microwave spectra of carbonyl sulfide: measurements of ground state and vibrationally excited $^{16}\text{O}^{13}\text{C}^{32}\text{S}$, $^{18}\text{O}^{12}\text{C}^{32}\text{S}$, and other isotopic species. *J Mol Spectrosc* 1973;47:226–33.
- [63] Burenin AV, Karyakin EN, Krupnov AF, Shapin SM, Val'dov AN. Submillimeter microwave spectrum and spectroscopic constants of the OCS molecule: less abundant isotopic species of the molecule. *J Mol Spectrosc* 1981;85:1–7.
- [64] Blanquet G, Walrand J, Courtoy CP, Fayt A. The ν_3 band of $^{16}\text{O}^{12}\text{C}^{34}\text{S}$ and $^{16}\text{O}^{13}\text{C}^{34}\text{S}$. *J Mol Spectrosc* 1980;81:473–9.
- [65] Hunt N, Foster SC, Johns JWC, McKellar ARW. High-resolution spectroscopy of 16 bands of OCS in the region 1975–2140 cm^{-1} for diode laser calibration. *J Mol Spectrosc* 1985;111:42–53.
- [66] Luiz GMRS, Scalabrin A, Pereira D. Gas phase infrared fourier transform spectra of H_12COOH and H_13COOH . *Infrared Phys Technol* 1997;38:45–9.
- [67] Baskakov OI, Markov IA, Alekseev EA, Motiyenko RA, Lohilahti J, Horneman V-M, Winnewisser BP, Medvedev IR, Lucia FCD. Simultaneous analysis of rovibrational and rotational data for the 4^1 , 5^1 , 6^1 , 7^2 , 8^1 , 7^1 , 9^1 and 9^2 states of HCOOH . *J Mol Struct* 2006;795:54–77.
- [68] Ong PP, Goh KL, Teo HH. Analysis of high-resolution FTIR spectrum of the ν_6 band of H_13COOH . *J Mol Spectrosc* 1999;194:203–5.
- [69] Zhao J, Billingham BE, Raston PL. Synchrotron-based pure rotational spectroscopy of H^{13}COOH . *J Quant Spectrosc Radiat Transf* 2024;312:108819.
- [70] Papoušek D, Winnewisser M, Klee S, Demaison J, Pracna P. Simultaneous rovibrational analysis of the ν_2 , ν_3 , ν_5 , and ν_6 bands of H_313CF . *J Mol Spectrosc* 1998;192:220–7.
- [71] Huang X, Gordon IE, Tashkun SA, Schwenke DW, Lee TJ. Accurate infrared line lists for 20 isotopologues of CS_2 at room temperature. *Astrophys J Suppl Ser* 2024; 272:17.
- [72] Karlovets EV, Gordon IE, Hashemi R, Kochanov RV, Hargreaves RJ, Rothman LS. Addition of the line list for carbon disulfide to the HITRAN database: line positions, intensities, and half-widths of the 12C32S2, 32S12C34S, 32S12C33S, and 13C32S2 isotopologues. *J Quant Spectrosc Radiat Transf* 2021;258:107275.
- [73] Bowersman CA, Mizus II, Zobov NF, Polyansky OL, Sarka J, Poirier B, Pezzella M, Yurchenko SN, Tennyson J. ExoMol line lists – L: high-resolution line lists of H_3^+ , H_2D^+ , D_2H^+ , and D_3^+ . *Mon Not R Astron Soc* 2023;519:6333–48.
- [74] Mizus II, Alijah A, Zobov NF, Lodi L, Kyuberis AA, Yurchenko SN, Tennyson J, Polyansky OL. ExoMol molecular line lists – XX. A comprehensive line list for H_3^+ . *Mon Not R Astron Soc* 2017;468:1717–25.
- [75] Neale L, Tennyson J. A high-temperature partition function for H_3^+ . *Astron J* 1915;454 (N. Y.)L169-L73.
- [76] Gomez FM, Hargreaves RJ, Gordon IE. A HITRAN-formatted UV line list of S_2 -containing transitions involving $\text{X}^3\Sigma_g^-$, $\text{B}^3\Sigma_u^-$, and $\text{B}^3\Pi_u$ electronic states. *Mon Not R Astron Soc* 2024;528:3823–32.
- [77] Perrin A, Demaison J, Toon G. The ν_1 , ν_2 , and ν_3 bands of carbonyl chlorofluoride (COFCl) at 5.3, 9.1, and 13.1 μm : position and intensity parameters and their use for atmospheric studies. *J Quant Spectrosc Radiat Transf* 2011;112:1266–79.
- [78] Perrin A, Flaud JM, Bürger H, Pawelke G, Sander S, Willner H. First high-resolution analysis of the six fundamental bands ν_1 , ν_2 , ν_3 , ν_4 , ν_5 , and ν_6 of COF_3Cl in the 340- to 2000- cm^{-1} region. *J Mol Spectrosc* 2001;209:122–32.
- [79] Dehayem-Kamadjeu A, Piralì O, Orphal J, Kleiner I, Flaud PM. The far-infrared rotational spectrum of nitrous acid (HONO) and its deuterated species (DONO) studied by high-resolution fourier-transform spectroscopy. *J Mol Spectrosc* 2005; 234:182–9.
- [80] Sironneau V, Flaud JM, Orphal J, Kleiner I, Chelin P. Absolute line intensities of HONO and DONO in the far-infrared and re-determination of the energy difference between the trans- and cis-species of nitrous acid. *J Mol Spectrosc* 2010;259:100–4.
- [81] McGraw GE, Bernitt DL, Hisatsune IC. Infrared spectra of isotopic nitrous acids. *J Chem Phys* 1966;45:1392–9.
- [82] Perrin A, Miljanic S, Dehayem-Kamadjeu A, Chélin P, Orphal J, Demaison J. The 14–22 μm absorption spectrum of nitrous acid studied by high-resolution fourier-transform spectroscopy: new analysis of the ν_5 and ν_6 interacting bands of trans-HONO and first analysis of the ν_6 band of cis-HONO. *J Mol Spectrosc* 2007;245: 100–8.
- [83] Guilmot JM, Godefroid M, Herman M. Rovibrational parameters for trans-nitrous acid. *J Mol Spectrosc* 1993;160:387–400.
- [84] Guilmot JM, Melen F, Herman M. Rovibrational parameters for cis-nitrous acid. *J Mol Spectrosc* 1993;160:401–10.
- [85] Allegrini M, Johns JWC, McKellar ARW, Pinson P. Stark spectroscopy with the CO laser: the ν_2 fundamental bands of trans- and cis-nitrous acid, HNO_2 , in the 6- μm region. *J Mol Spectrosc* 1980;79:446–54.
- [86] Deeley CM, Mills IM. The infrared vibration—rotation spectrum of trans and cis nitrous acid. *J Mol Struct* 1983;100:199–213.
- [87] Deeley CM, Mills IM, Halonen LO, Kauppinen J. Vibration—rotation spectra of nitrous acid, HONO. *Can J Phys* 1985;63:962–5.
- [88] Betnga WT, Tchana FK, Perrin A, Manceron L, Auwera JV, Hindle F, Coutens A. New line intensities for the far infrared bands of the trans- and Cis-conformer of nitrous acid (HONO), new determination of the trans-Cis conformer barrier and its impact on the astrophysical detection of nitrous acid in protostellar clouds. *J Quant Spectrosc Radiat Transf* 2023;310:108727.
- [89] Pickett HM, Cohen EA, Drouin BJ, Pearson JC. Submillimeter, millimeter, and microwave spectral line catalog. Pasadena, CA: Jet Propulsion Laboratory; 2003.
- [90] Shimanouchi T. Tables of molecular vibrational frequencies consolidated volume 1. *Natl Stand Ref Data Ser* 1972;39:1–161.
- [91] Flaud JM, Anantharajah A, Tchana FK, Manceron L, Orphal J, Wagner G, Birk M. High-resolution analysis of the 12.6 μm spectral region of the nitril chloride ClNO_2 molecule. *J Quant Spectrosc Radiat Transf* 2019;224:217–21.
- [92] Anantharajah A, Kwabia Tchana F, Manceron L, Orphal J, Flaud JM. New analysis of line positions of the ν_3 bands of $^{35}\text{ClNO}_2$ and $^{37}\text{ClNO}_2$ around 370 cm^{-1} . *J Quant Spectrosc Radiat Transf* 2020;253:107078.
- [93] Orphal J, Morillon-Chapey M, Klee S, Mellau GC, Winnewisser M. The far-infrared spectrum of ClNO_2 studied by high-resolution fourier-transform spectroscopy. *J Mol Spectrosc* 1998;190:101–6.
- [94] Kochanov RV, Gordon IE, Rothman LS, Wcislo P, Hill C, Wilzewski JS. HITRAN application programming interface (HAPI): a comprehensive approach to working with spectroscopic data. *J Quant Spectrosc Radiat Transf* 2016;177:15–30.